

Experiments with K-Meson Decays

T. K. Komatsubara

High Energy Accelerator Research Organization (KEK), Japan

submitted on December 1, 2011

revised on March 19, 2012

Abstract

Recent results and future prospects of the particle physics experiments with neutral and charged K-meson (kaon) decays are reviewed. Topics include CP violation, rare decays, leptons in kaon decays, tests of CPT and quantum mechanics, radiative decays, hadrons in kaon decays, basic observables, V_{us} and CKM unitarity, and exotic searches. Experimental techniques developed for the kaon decay experiments are discussed.

1 Introduction

K-mesons (kaons) were discovered in 1947 in “two (cloud-chamber) photographs (of cosmic ray showers) containing forked tracks of a very striking character” [1]. They were the first heavy-flavor particles, which can be produced by strong interactions but have only weak decays. Through the decays they had major contributions [2] toward establishing the Standard Model (SM) of particle physics. In the modern experiments, with millions of kaon decays per second by high-intensity accelerators, searches and measurements with the sensitivity of $10^{-8} \sim 10^{-12}$ are performed and the flavor parameters in and beyond the SM are studied.

In this article ¹, recent results and future prospects of kaon decay experiments (table 1) are reviewed. Emphasis is placed on the achievements in the first decade of this century. Theoretical kaon physics is not fully covered because comprehensive reviews are available (e.g. [6, 7, 8, 9]).

Reminder: the experimental upper limits in this article are at the 90% confidence level (C.L.).

¹ The materials in my previous reviews [3, 4, 5] are expanded and updated.

Table 1: Kaon decay experiments being reviewed in this article.

Lab	Accelerator	Experiment	Kaon decay
KEK	KEK-PS (12 GeV)	E246 ✓ E391a ✓	K^+ at rest K_L^0
BNL	AGS (25 GeV)	E949 ✓, E787 ✓	K^+ at rest
KEK - JAEA ^a	J-PARC Main Ring (30 GeV)	K ^O TO TREK	K_L^0 K^+ at rest
IHEP, Protvino	U-70 (70 GeV)	ISTRA+ ✓ OKA	K^- in flight K^\pm in flight
CERN	SPS (400 GeV)	NA48 ✓ NA48/1 ✓ NA48/2 ✓ NA62	K_L^0, K_S^0 K_S^0 K^\pm in flight K^+ in flight
FNAL	Tevatron (800 GeV)	KTeV ✓	K_L^0, K_S^0
INFN, Frascati	DAΦNE ($\sqrt{s} \sim 1.02\text{GeV}$)	KLOE✓ KLOE-2	$K_L^0 + K_S^0, K^+ + K^-$ $K_L^0 + K_S^0, K^+ + K^-$

^a JAEA is the abbreviation of Japan Atomic Energy Agency.

✓ Data taking of the experiment is completed.

Table 2: Modern classification of CP violation.

	example	hadronic uncertainties	kaon decays
mixing	semileptonic decay $\frac{\Gamma(\overline{M}^0(t) \rightarrow \ell^+ \nu X) - \Gamma(M^0(t) \rightarrow \ell^- \overline{\nu} X)}{\Gamma(M^0(t) \rightarrow \ell^+ \nu X) + \Gamma(M^0(t) \rightarrow \ell^- \overline{\nu} X)}$	form factors	$K^0 \rightarrow \pi \mu \nu, \pi e \nu$ ✓
decay	hadronic decay $M \rightarrow f \text{ vs. } \overline{M} \rightarrow \overline{f}$ $\frac{\Gamma(M^- \rightarrow f) - \Gamma(M^+ \rightarrow \overline{f})}{\Gamma(M^- \rightarrow f) + \Gamma(M^+ \rightarrow \overline{f})}$	hadronic matrix elements, strong phases	$K^0 \rightarrow \pi \pi$ ✓ K^\pm decays
interference between decays w/ and w/o mixing	$M^0 \rightarrow f_{CP}$ and $\overline{M}^0 \rightarrow \overline{f}_{CP}$ $\frac{\Gamma(\overline{M}^0(t) \rightarrow f) - \Gamma(M^0(t) \rightarrow \overline{f})}{\Gamma(\overline{M}^0(t) \rightarrow f) + \Gamma(M^0(t) \rightarrow \overline{f})}$	form factors, possible long-distance effects	$K_L^0 \rightarrow \pi^0 \nu \overline{\nu}$

✓ The CP violation has been observed.

f_{CP} : CP eigenstate

2 CP Violation

2.1 Overview

The CP-violating $K_L^0 \rightarrow \pi^+ \pi^-$ decay was discovered [10], unexpectedly, in 1964 at the sensitivity of 10^{-3} . After the CP asymmetry in the $K^0 - \overline{K}^0$ mixing, with the parameter ϵ , was established [11, 12], a long-standing problem has been its origin; the first question was whether it was due to the $\Delta S = 2$ *superweak* transition [13] or not. In 1973, Kobayashi and Maskawa [14] accommodated CP violation in the electroweak theory with six quarks (and a single complex-phase in the mass-eigenstate mixing matrix under the charged-current interactions). The Kobayashi-Maskawa theory [15, 16], including the prediction of *direct* CP violation in the decay process from the CP-odd component (K_2) to the CP-even state ($\pi\pi$), was verified by the observations of Time-reversal non-invariance (CPLEAR [17] at CERN) and finally due to the determination of ϵ'/ϵ (NA48 at CERN and KTeV at FNAL) as well as the discoveries of top quark and CP-violating B-meson decays.

In the modern classification (e.g. [18]) CP violation is grouped into three: in *mixing*, *decay*, and *interference between decays with and without mixing* (table 2). All of these have been extensively studied in the B Factory experiments. Experimental studies in neutral-kaon decays have a long history, while the study of CP violation in the charged-kaon decay modes started recently. The CP-violating processes in *mixing* and *decay* suffer from hadronic uncertainties. A rare decay $K_L^0 \rightarrow \pi^0 \nu \overline{\nu}$ [19], which will be discussed in Section 3.2, is known to be a golden mode in this category [20] because the branching ratio can be calculated with very small theoretical-uncertainties in the SM as well as in its extensions.

The rest of this section is devoted to the kaon results of the CP violation in *decay*.

2.2 CP Violation in decay

The NA48 collaboration at CERN and the KTeV collaboration at FNAL published the final measurement of $Re(\epsilon'/\epsilon)$ as $(14.7 \pm 2.2) \times 10^{-4}$ [21] and $(19.2 \pm 2.1) \times 10^{-4}$ [22], respectively, where $Re(\epsilon'/\epsilon)$ is

obtained from the double ratio of decay rates:

$$\frac{\Gamma(K_L^0 \rightarrow \pi^0 \pi^0) / \Gamma(K_S^0 \rightarrow \pi^0 \pi^0)}{\Gamma(K_L^0 \rightarrow \pi^+ \pi^-) / \Gamma(K_S^0 \rightarrow \pi^+ \pi^-)} \approx 1 - 6 \operatorname{Re}(\epsilon'/\epsilon) \quad (1)$$

or

$$\frac{\Gamma(K_L^0 \rightarrow \pi^+ \pi^-) / \Gamma(K_S^0 \rightarrow \pi^+ \pi^-)}{\Gamma(K_L^0 \rightarrow \pi^0 \pi^0) / \Gamma(K_S^0 \rightarrow \pi^0 \pi^0)} \approx 1 + 6 \operatorname{Re}(\epsilon'/\epsilon) . \quad (2)$$

The detectors for $\operatorname{Re}(\epsilon'/\epsilon)$ [23, 24, 25] are shown in Fig. 1. All the four decay modes have to be measured simultaneously and with high precisions (in particular to $K_L^0 \rightarrow \pi^0 \pi^0$); thus, a novel technique of double beams and a state-of-the-art electromagnetic calorimeter were developed. The NA48 experiment, shown in Fig. 1 top, used two target stations for kaon production ² and the liquid-Krypton (LKr) electromagnetic calorimeter of 27 radiation-length (X_0) deep. The KTeV experiment, shown in Fig. 1 bottom, used side-by-side identical K_L^0 beams with the regenerator alternating between them ³ and the undoped cesium iodide (CsI) calorimeter of $27X_0$ long. Combining all the recent measurements of $\operatorname{Re}(\epsilon'/\epsilon)$ in Fig. 2, the world average is $(16.8 \pm 1.4) \times 10^{-4}$ [26]; it clearly demonstrates the existence of the CP violation in *decay*. However, due to theoretical uncertainties in the hadronic matrix elements, to get information on the SM and New Physics beyond it from $\operatorname{Re}(\epsilon'/\epsilon)$ is difficult and remains to be a challenge to theoretical calculations.

The NA48/2 collaboration at CERN performed charge asymmetry measurements with the simultaneous K^+ and K^- beams (Fig. 3), overlapping in space, of 60 ± 3 GeV/c in 2003 and 2004. The $K^\pm \rightarrow \pi^\pm \pi \pi$ matrix element squared (Dalitz-plot density) is parametrized [27] by a polynomial expansion with two Lorentz-invariant kinematic variables u and v :

$$|M(u, v)|^2 \propto 1 + g \cdot u + h \cdot u^2 + k \cdot v^2 , \quad (3)$$

where the coefficients g , h , k are called as the linear and quadratic *slope parameters*. The linear slope parameters, g^+ and g^- , describe the decays of K^+ and K^- , respectively, and the slope asymmetry $A_g = (g^+ - g^-)/(g^+ + g^-)$ is a manifestation of CP violation in *decay*. The asymmetries of the $K^\pm \rightarrow \pi^\pm \pi^+ \pi^-$ decay A_g^c and the $K^\pm \rightarrow \pi^\pm \pi^0 \pi^0$ decay A_g^n were measured to be $A_g^c = (-1.5 \pm 2.2) \times 10^{-4}$ and $A_g^n = (1.8 \pm 1.8) \times 10^{-4}$ with the data sets of 4G and 0.1G events, respectively [28]. The SM expectation is in $10^{-5} \sim 10^{-6}$, and no evidence for CP violation in *decay* was observed in the K^\pm decays at the level of 2×10^{-4} . The NA48/2 experiment also measured the asymmetries of K^+ and K^- decay-rates in $K^\pm \rightarrow \pi^\pm e^+ e^-$, $K^\pm \rightarrow \pi^\pm \mu^+ \mu^-$ and $K^\pm \rightarrow \pi^\pm \pi^0 \gamma$ to be $(-2.2 \pm 1.5(\text{stat.}) \pm 0.6(\text{syst.})) \times 10^{-2}$ [29], $(1.2 \pm 2.3) \times 10^{-2}$ [30] and $(0.0 \pm 1.0(\text{stat.}) \pm 0.6(\text{syst.})) \times 10^{-3}$ [31] and set the upper limits of 2.1%, 2.9% and 0.15%, respectively.

No new plan for the $\operatorname{Re}(\epsilon'/\epsilon)$ and A_g measurements is being proposed.

² A proton beam extracted from SPS hit one target for K_L^0 , and a lower-intensity proton beam, which was selected by channelling the protons not interacting in the K_L^0 target in a bent silicon crystal, was transported to a second target for K_S^0 close to the detector. A time coincidence between an observed decay and a tagging counter, which was crossed by the low intensity proton beam on its way to the K_S^0 target, was used to identify the decay as coming from a K_S^0 rather than a K_L^0 .

³ The regenerator created a coherent $|K_L^0 \rangle + \rho |K_S^0 \rangle$ state, where ρ is the regeneration amplitude. Most of the $K \rightarrow \pi \pi$ decay rate downstream of the regenerator is from the K_S^0 component.

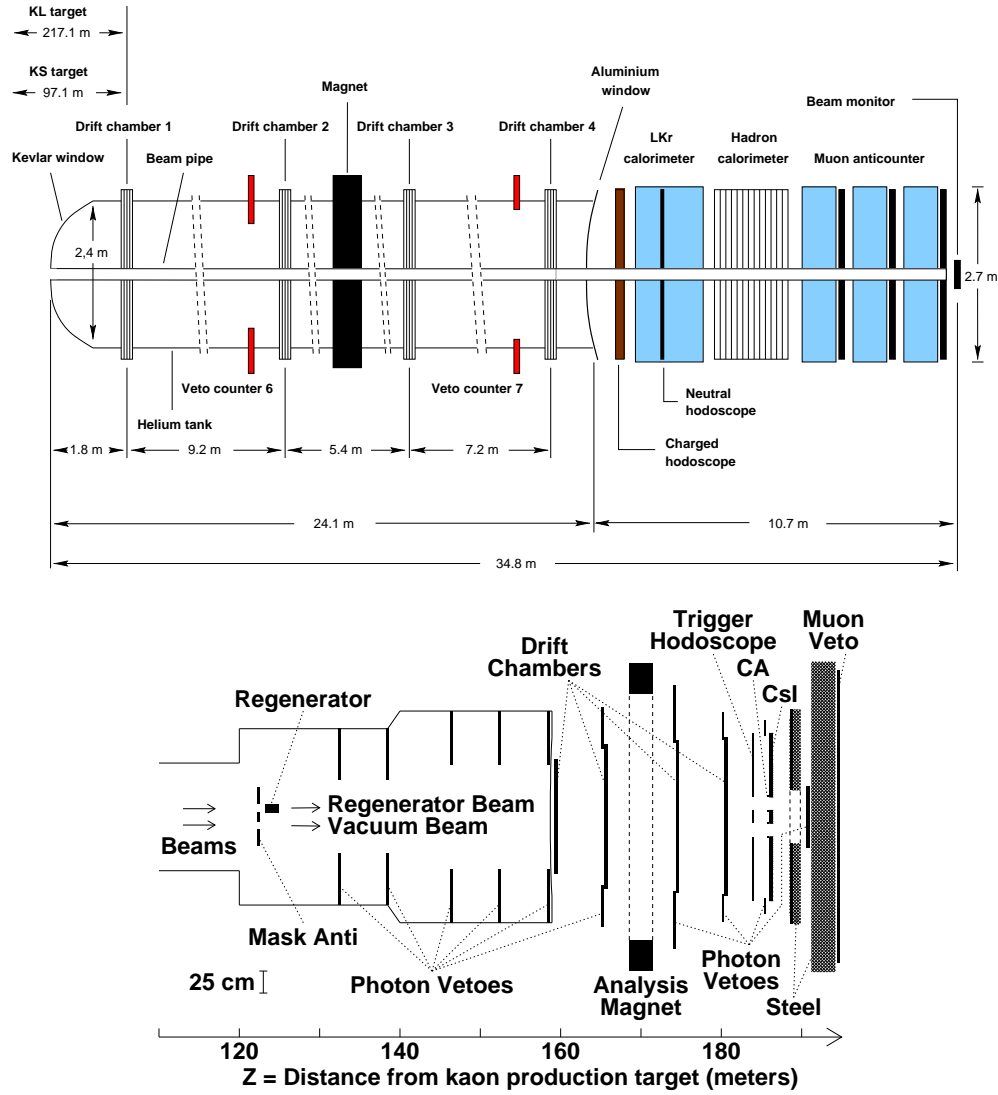


Figure 1: The NA48 detector with a magnetic spectrometer consisting of four drift chambers and a dipole magnet and a scintillator hodoscope for charged particles, a liquid-Krypton calorimeter for photons, and an iron-scintillator calorimeter and a series of muon counters for charged-particle identification (top); the KTeV detector with a regenerator, a magnetic spectrometer and a hodoscope, a cesium iodide calorimeter, and a muon counter (bottom). Both detectors had a system of counters surrounding the fiducial region to detect photons escaping the acceptance of the calorimeter. Source: Figures taken from Refs.[24, 22].

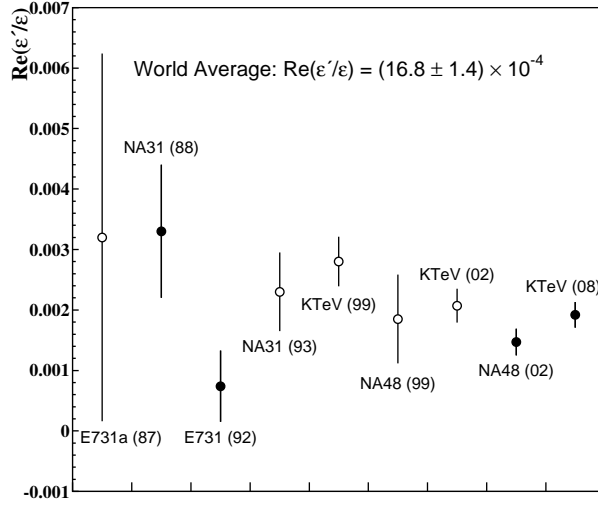


Figure 2: Recent measurements of $Re(\epsilon'/\epsilon)$. Source: Figure taken from Ref.[26].

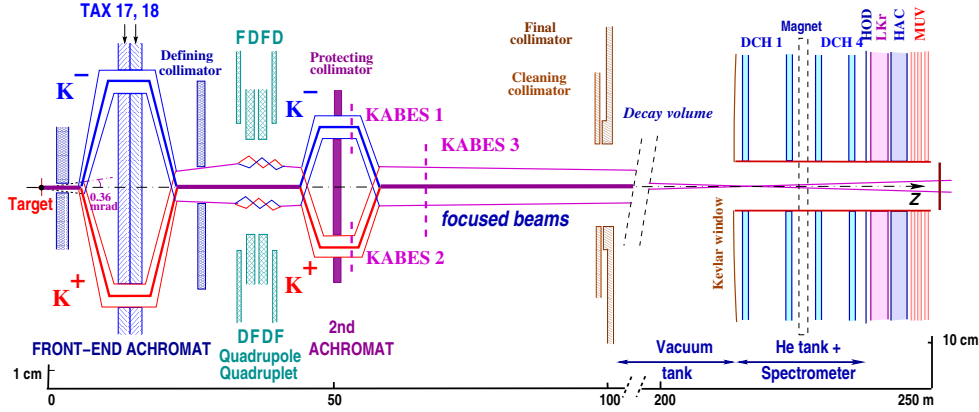


Figure 3: Schematic side view of the NA48/2 beam line, decay volume and detector. TAX17, 18: motorized beam dump/collimators used to select the momentum of the K^+ and K^- beams; FDFD/DFDF: focusing magnets; KABES 1-3: kaon beam spectrometer stations. DCH 1-4: drift chambers; HOD: hodoscope; LKr: calorimeter; HAC: hadron calorimeter; MUV: muon veto. Source: Figure taken from Ref.[28].

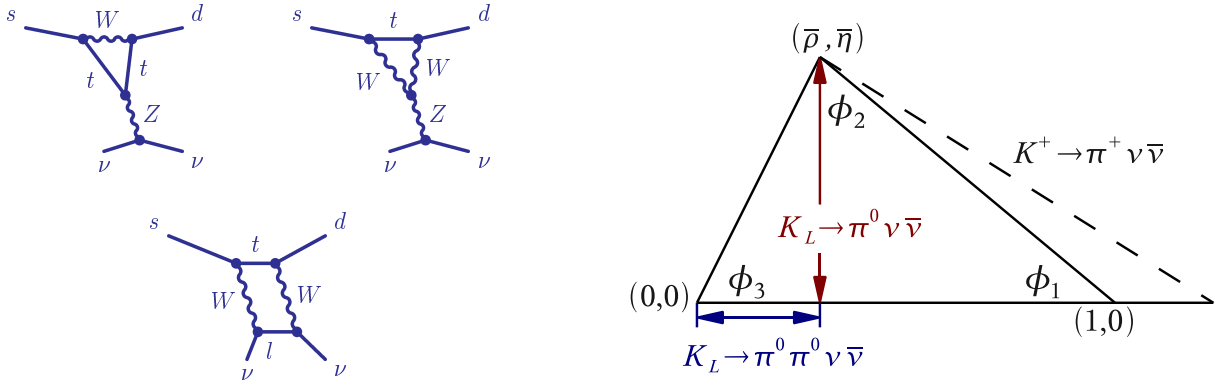


Figure 4: SM diagrams for $K \rightarrow \pi \nu \bar{\nu}$ (left); kaon unitarity triangle in the (ρ, η) plane (right).

3 Rare decays

3.1 Overview

A famous contribution of kaon physics to the SM was the absence of the decays due to Flavor-Changing Neutral Current (FCNC), $K_L^0 \rightarrow \mu^+ \mu^-$, $K^+ \rightarrow \pi^+ e^+ e^-$ and $K^+ \rightarrow \pi^+ \nu \bar{\nu}$, in 1960's. The Glashow-Iliopoulos-Maiani (GIM) mechanism [32] explained it [33] with the the unitarity matrix for mass-eigenstate mixing in advance of the charm-quark discovery in 1974. The next theoretical milestone was the Inami-Lim loop functions [34] in 1981 for FCNC processes with heavy quark and leptons. In addition to the continual searches for decays at higher levels than the SM predictions, the anticipation of detecting rare kaon decays in the SM range got more and more realistic with the rise of the top-quark mass. The evidence for the $K^+ \rightarrow \pi^+ \nu \bar{\nu}$ decay [35] by the E787 collaboration at BNL in 1997 opened a new era of testing the SM by measuring rare processes.

The FCNC process in kaon decays is strange-quark to down-quark transition and is induced in the SM by the electroweak loop effects as Penguin and Box diagrams (Fig. 4 left). The top-quark in the loops dominates the transition because of its heavy mass, and the quantity:

$$\lambda_t \equiv V_{ts}^* \cdot V_{td} = -A^2 \lambda^5 \cdot (1 - \rho - i\eta) = -|V_{cb}|^2 \cdot \lambda \cdot (1 - \rho - i\eta), \quad (4)$$

where $\lambda \equiv |V_{us}| \simeq 0.225$ (to be discussed in Section 9), is measured. λ , A , ρ , and η are the Wolfenstein parametrization [36] of the Cabibbo-Kobayashi-Maskawa (CKM) matrix [37, 14]. The decays are rare due to $|V_{cb}|^2 \cdot \lambda$, and are precious because the important parameters ρ and η can be determined from them. The decay amplitude of K_L^0 is a superposition of the amplitudes of K^0 and \bar{K}^0 and is proportional to η ; thus, observation of a rare K_L^0 decay to a CP-even state is a new evidence for CP violation.

We start with $K_L^0 \rightarrow \pi^0 \nu \bar{\nu}$ and the charged counterpart $K^+ \rightarrow \pi^+ \nu \bar{\nu}$, because measurement of their branching ratios is currently the main issue of kaon physics [38].

3.2 $K \rightarrow \pi \nu \bar{\nu}$

The branching ratios of the $K \rightarrow \pi \nu \bar{\nu}$ decays [39] are predicted in the SM, to an exceptionally high degree of precision, as [40]

$$B(K_L^0 \rightarrow \pi^0 \nu \bar{\nu}) = \kappa_L \left(\text{Im} \frac{\lambda_t}{\lambda^5} \cdot X_t \right)^2 \quad (5)$$

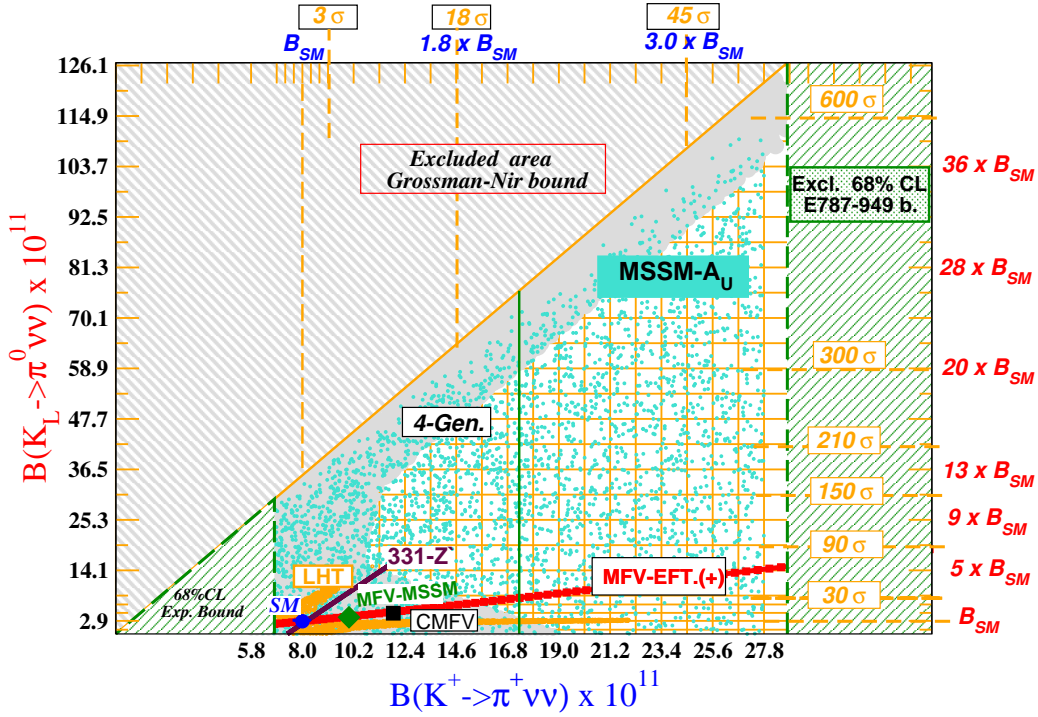


Figure 5: $K_L^0 \rightarrow \pi^0 \nu \bar{\nu}$ branching ratio versus $K^+ \rightarrow \pi^+ \nu \bar{\nu}$ branching ratio plot of the theoretical predictions in the Standard Model (SM) and in its extensions such as the minimal flavor violation (MFV), constrained minimal flavor violation (CMFV), minimal Supersymmetric Standard Model (MSSM), littlest Higgs model with T-parity (LHT), minimal 3-3-1 model (331-Z'), and four-generation model (4-Gen.). Excluded areas by the measured $K^+ \rightarrow \pi^+ \nu \bar{\nu}$ branching ratio and the model-independent bound due to their isospin relation are also shown in the plot. Source: Figure taken from Ref.[45].

$= 2.43 \text{ (39) (06)} \times 10^{-11}$ and

$$B(K^+ \rightarrow \pi^+ \nu \bar{\nu}(\gamma)) = \kappa_+ (1 + \Delta_{\text{EM}}) \left[\left(\text{Im} \frac{\lambda_t}{\lambda^5} \cdot X_t \right)^2 + \left(\text{Re} \frac{\lambda_t}{\lambda^5} \cdot X_t + \text{Re} \frac{\lambda_c}{\lambda} \cdot (P_c + \delta P_{c,u}) \right)^2 \right] \quad (6)$$

$= 7.81 \text{ (75) (29)} \times 10^{-11}$. The first error summarizes the parametric uncertainties dominated by $|V_{cb}|$, ρ and η , and the second error summarizes the remaining theoretical uncertainties. Long-distance contributions to $K \rightarrow \pi \nu \bar{\nu}$ are small; the hadronic matrix elements contained in the parameters κ_L and κ_+ can be extracted from the $K_{\ell 3}$ decays (Section 8), and the long-distance QED corrections are denoted by Δ_{EM} [41]. λ_t/λ^5 and λ_c/λ , where $\lambda_c \equiv V_{cs}^* \cdot V_{cd}$, represent the CKM-matrix parameters in $K \rightarrow \pi \nu \bar{\nu}$ and are in $O(\lambda^0)$. The decay amplitudes of $K_L^0 \rightarrow \pi^0 \nu \bar{\nu}$ and $K^+ \rightarrow \pi^+ \nu \bar{\nu}$ are proportional to the height (and thus the area) and the length of a side of the CKM unitarity triangle, respectively, giving access to the parameters ρ and η as shown in Fig. 4 right. The function X_t is the top-quark contribution to $K \rightarrow \pi \nu \bar{\nu}$; the complete two-loop electroweak corrections to X_t [40] as well as the next-to-next-to-leading order QCD corrections [42] and the QED and electroweak corrections [43] to the charm quark contribution to $K^+ \rightarrow \pi^+ \nu \bar{\nu}$, parametrized by P_c and $\delta P_{c,u}$, have been calculated.

New Physics could affect these branching ratios [44, 45, 46, 47, 48] and, by the measurement, the flavor structure in New Physics (operators and phases in the interactions of new particles) can be studied. The $K \rightarrow \pi \nu \bar{\nu}$ branching ratios beyond the Standard Model are presented in Fig. 5. A model-independent bound $B(K_L^0 \rightarrow \pi^0 \nu \bar{\nu}) < 4.4 \times B(K^+ \rightarrow \pi^+ \nu \bar{\nu})$, called the Grossman-Nir bound [20], can

be extracted from their isospin relation.

The signature of $K \rightarrow \pi\nu\bar{\nu}$ is a kaon decay into a pion plus *nothing*. Background rejection is essential in the experiments, and *blind analysis* techniques have been developed and refined to achieve a high level of confidence in the background measurements. To verify *nothing*, hermetic extra-particle detection by photon and charged-particle detectors, called the *veto* as a jargon in the experiments, is imposed to the hits in coincidence with the pion time and with the visible-energy threshold less than a few MeV. Tight veto requirements are indispensable in order to achieve a low detection-inefficiency $< 10^{-3} \sim 10^{-4}$; good timing resolution for low energy hits is therefore essential to avoid acceptance loss due to accidental hits in the environment of high-intensity beam.

The E391a collaboration at KEK performed the first dedicated search for the $K_L^0 \rightarrow \pi^0\nu\bar{\nu}$ decay. A well-collimated, small-diameter neutral beam (called a *pencil* beam [49], Fig. 6 top) was designed and constructed. The K_L^0 beam, whose momentum peaked at 2 GeV/c, was produced by the 12-GeV protons of KEK-PS. The E391a detector is shown in Fig. 6 bottom. The energy and position of the two photons from π^0 decays were measured by a downstream electromagnetic calorimeter consisting of 576 undoped-CsI crystals in the size of $7.0 \times 7.0 \times 30$ cm³ (i.e. $16X_0$ long) [50]. Assuming that the invariant mass of two photons was equal to the π^0 mass and that the decay vertex was on the beam axis, the K_L^0 -decay vertex position, Z_{vtx} , and the transverse momentum of π^0 , P_T , were determined. A π^0 with a large transverse momentum ($P_T \geq 0.12$ GeV/c) was the signal. In order to suppress the major background from $K_L^0 \rightarrow \pi^0\pi^0$, the remaining part of the calorimeter not hit by the two photons as well as all the other detector subsystems covering the decay region [51, 52] were used as a veto. The beam line and the collimation scheme were designed carefully to minimize the beam halo (mostly neutrons), which could interact with the counters near the beam and produce π^0 's and η 's.

In the final results from E391a on $K_L^0 \rightarrow \pi^0\nu\bar{\nu}$ [53], the single event sensitivity was 1.11×10^{-8} and no events were observed inside the signal region (Fig. 7). The upper limit on $B(K_L^0 \rightarrow \pi^0\nu\bar{\nu})$ was set to be 2.6×10^{-8} . The E391a experiment has improved the limit from previous experiments (5.9×10^{-7} [54] using $\pi^0 \rightarrow e^+e^-\gamma$)⁴ by a factor of 23. E391a also obtained an upper limit of 8.1×10^{-7} [56] for the branching ratio of the $K_L^0 \rightarrow \pi^0\pi^0\nu\bar{\nu}$ decay, which is a CP conserving process and is sensitive to $\text{Re}\lambda_t$ (Fig. 4 right).

The E949 and E787 collaborations at BNL measured the charged track emanating from $K^+ \rightarrow \pi^+\nu\bar{\nu}$ decaying at rest in the stopping target. The Low Energy Separated Beam line (LESB III [57], Fig. 8 top) of AGS transported K^+ 's with momentum 0.7 GeV/c to the detector (Fig. 8 bottom). Pion contamination to the incident K^+ beam was reduced, to a $K^+ : \pi^+$ ratio of 4 : 1, by two stages of electrostatic particle separation in LESB III to prevent that scattered beam pions would contribute to the background. Charged-particle detectors for measurement of the π^+ properties were located in the central region of the detector and were surrounded by hermetic photon detectors. The π^+ momentum (P_{π^+}) from $K^+ \rightarrow \pi^+\nu\bar{\nu}$ is less than 0.227 GeV/c, while the major background sources of $K^+ \rightarrow \pi^+\pi^0$ and $K^+ \rightarrow \mu^+\nu$ are two-body decays and have monochromatic momentum of 0.205 GeV/c and 0.236 GeV/c, respectively. Two signal regions with the π^+ momentum above and below the peak from $K^+ \rightarrow \pi^+\pi^0$ were adopted. Redundant kinematic measurement and μ^+ rejection were employed; the latter was crucial in the trigger as well as in the offline analysis because the $K^+ \rightarrow \mu^+\nu$ background had the same topology as the signal.

The E949 experiment observed one $K^+ \rightarrow \pi^+\nu\bar{\nu}$ event in the kinematic region $0.211 < P_{\pi^+} < 0.229$ GeV/c (PNN1) [58] and three events in the region $0.140 < P_{\pi^+} < 0.199$ GeV/c (PNN2) [59]. Combining the results with the observation of two events in PNN1 and one event in PNN2 by the predecessor E787 experiment, a branching ratio of $B(K^+ \rightarrow \pi^+\nu\bar{\nu}) = (1.73_{-1.05}^{+1.15}) \times 10^{-10}$ (Fig. 9) [59] was obtained and was consistent with the Standard Model prediction. The upper limit $B(K^+ \rightarrow \pi^+\nu\bar{\nu}) < 3.35 \times 10^{-10}$ was also determined and can be used to calculate the Grossman-Nir bound on $B(K_L^0 \rightarrow \pi^0\nu\bar{\nu})$ as

⁴ The improvement from the limit using $\pi^0 \rightarrow \gamma\gamma$, 1.6×10^{-6} [55], is a factor of 62.

1.46×10^{-9} , which is smaller than the limit by E391a. The E787 experiment also obtained an upper limit of 4.3×10^{-5} [60] for the branching ratio of the $K^+ \rightarrow \pi^+ \pi^0 \nu \bar{\nu}$ decay.

The next generation of $K_L^0 \rightarrow \pi^0 \nu \bar{\nu}$ is the E14 K^OTO experiment [61, 62, 63] at the new high-intensity proton accelerator facility J-PARC (Japan Proton Accelerator Research Complex) [64]. The accelerators consist of a Linac, 3-GeV Rapid Cycle Synchrotron and Main Ring, and the physics program with slow and fast beam-extractions of 30 GeV protons has started ⁵. The K^OTO collaboration built the new neutral beam-line [66] (Fig. 10) at the Hadron Experimental Hall [67] of J-PARC and surveyed the beam [68, 69] in 2009. They constructed a new electromagnetic calorimeter in 2010 with the 27X₀-long undoped-CsI crystals ⁶, used in the past in the KTeV experiment, and started a commissioning ⁷. They will continue the detector construction in 2012 and expect to start the physics run in 2013. The detector subsystems in E391a are reused or upgraded; in particular, the collar-shaped photon counter at the entrance of the decay region (CC02 in Fig. 6 bottom) will be made of CsI crystals and renamed as Neutron Collar Counter, so as to be with the capability of measuring neutrons in the beam halo, and the counter to identify charged particles in front of the calorimeter (CV in Fig. 6 bottom) will be made by plastic-scintillator strips. The photon counter to cover the beam hole (BA in Fig. 6 bottom) will be replaced by an array of aerogel Čerenkov counters with lead converters; the counters are designed to be insensitive to neutrons while keeping a high detection efficiency for photons. The trigger and data acquisition systems are newly built by introducing the schemes of waveform digitization and pipe-line readout. As the first step in measuring $B(K_L^0 \rightarrow \pi^0 \nu \bar{\nu})$ at J-PARC, K^OTO aims at the first observation of the $K_L^0 \rightarrow \pi^0 \nu \bar{\nu}$ decay at the SM sensitivity.

The next generation of $K^+ \rightarrow \pi^+ \nu \bar{\nu}$ is the NA62 experiment [70, 71] at CERN, which will use K^+ decays in flight from an un-separated beam of 75 GeV/*c* from SPS. The construction of the NA62 detector [72, 73] (Fig. 11) is proceeding steadily. The incoming kaon is measured by the Gigatracker system in the beam. The charged decay particle is measured by the straw-chamber spectrometer and is identified by the Ring Imaging Čerenkov (RICH) detector and the muon-veto sampling calorimeter. The LKr calorimeter, originally built for NA48, is used as a veto for forward photons. Photons at large angles are intercepted by a series of 12 ring-shaped veto counters constructed using lead-glass blocks from the OPAL electromagnetic barrel calorimeter. A technical run will be made in the autumn of 2012 before the long shut-down of LHC. Given CERN's current accelerator-operation plan, first physics for NA62 is expected in 2014 or 2015. The goal of NA62 is to detect 100 $K^+ \rightarrow \pi^+ \nu \bar{\nu}$ events with no more than 10% background.

In the US, a new experiment to measure $B(K^+ \rightarrow \pi^+ \nu \bar{\nu})$ with K^+ decays at rest is proposed to FNAL (P1021 ORKA). Higher sensitivity kaon experiments based on a new high-intensity proton source at FNAL [74, 75] are now under discussion [76].

⁵ Proposals for particle and nuclear physics experiments at J-PARC are available from [65].

⁶ The K^OTO calorimeter consists of 2240 small CsI blocks, in the size of $2.5 \times 2.5 \times 50$ cm³, for the central region and 476 large CsI blocks, in the size of $5.0 \times 5.0 \times 50$ cm³, for the outer region.

⁷ J-PARC was affected by the East Japan Earthquake on March 11, 2011, but there was no effect of Tsunami that happened nearby and no one was injured. The beam line and the calorimeter for K^OTO was not damaged. The J-PARC accelerators started re-commissioning in December 2011 and resumed the operation in January 2012.

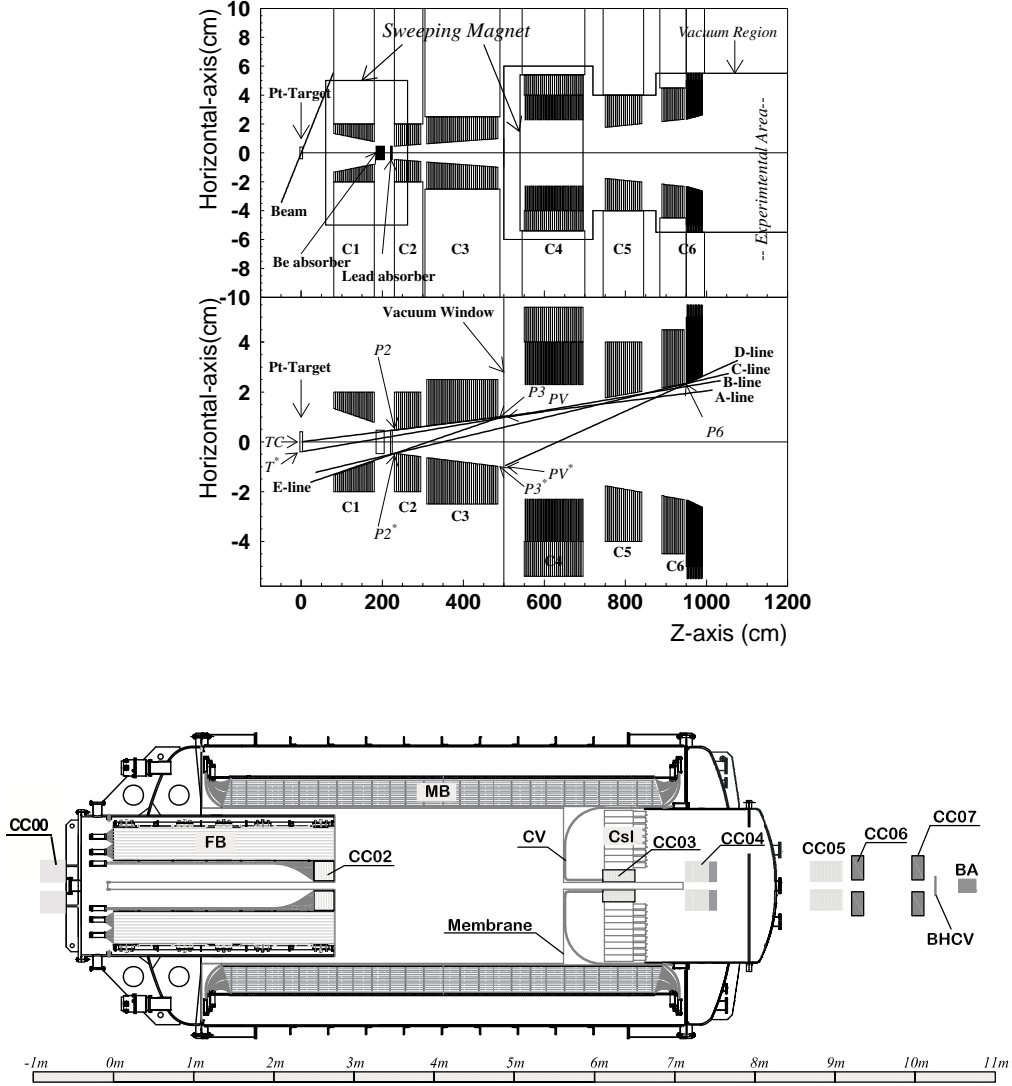


Figure 6: Schematic horizontal views of the neutral beam line for E391a: the arrangements of the components including six collimators C1-C6, and the collimation scheme (top); cross-sectional view of the E391a detector (bottom). CsI: electromagnetic calorimeter; CV: charged-particle counter; MB and FB: main-barrel and front-barrel photon counters; CC00, CC02-CC07: collar-shaped photon counters; BHCV and BA: beam hole charged-particle and photon counters. Source: Figures taken from Refs.[49, 53].

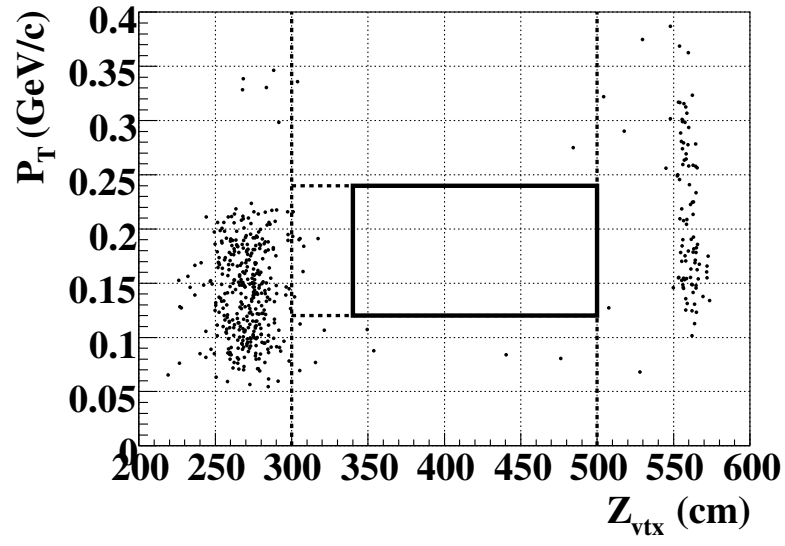


Figure 7: E391a result on $K_L^0 \rightarrow \pi^0 \nu \bar{\nu}$. Source: Figure taken from Ref.[53].

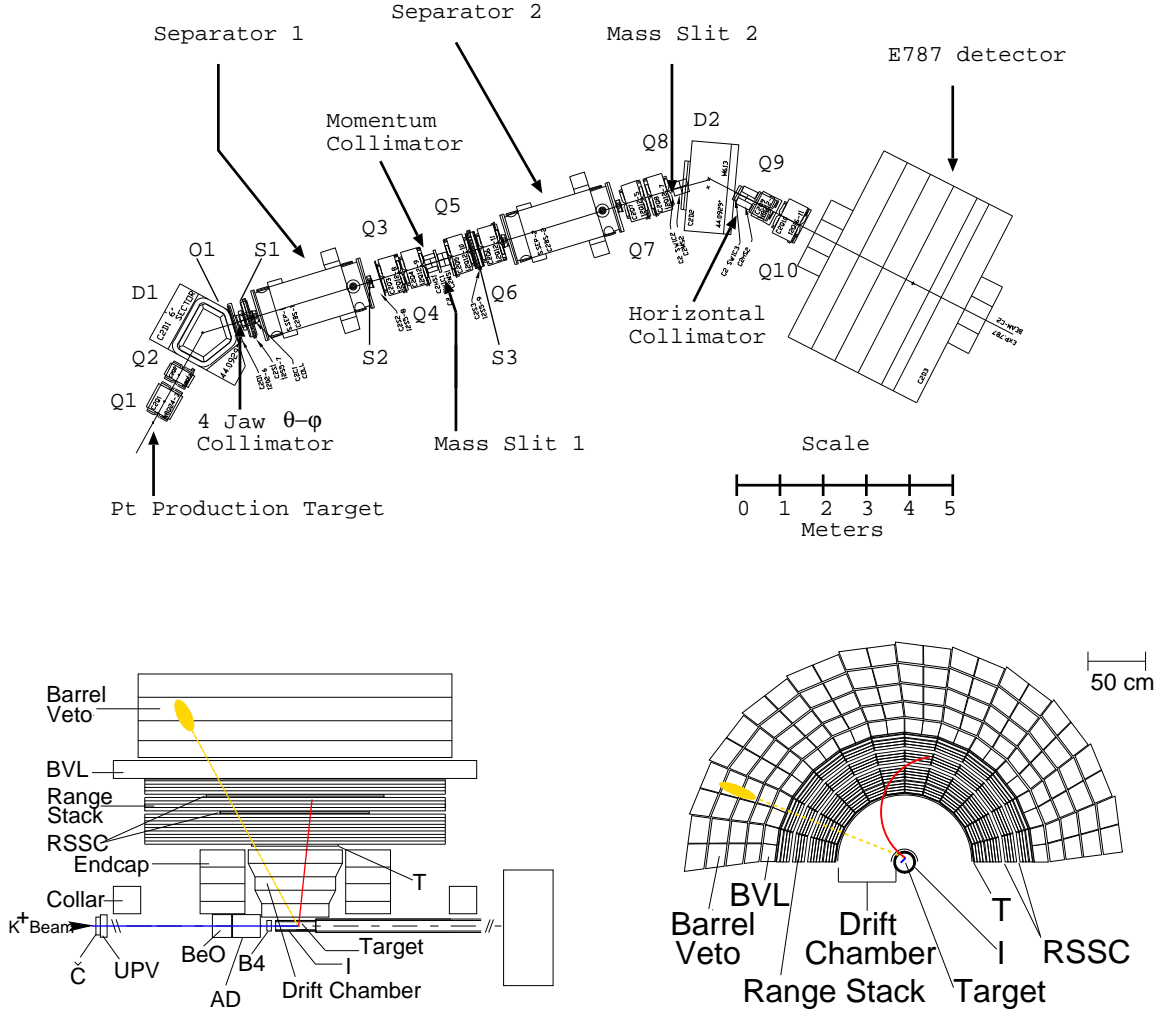


Figure 8: Layout of LESB III of AGS for the E949/E787 experiment with two dipole (D1,D2), ten quadrupole (Q1-Q10), three sextupole (S1-S3) and one octupole (O1) magnets (top); schematic side (bottom left) and end (bottom right) views of the upper half of the E949 detector. The outgoing charged pion and one photon from $\pi^0 \rightarrow \gamma\gamma$ decay are illustrated. \check{C} : Čerenkov counter; B4: energy-loss counters; I and T: inner and outer trigger scintillation counters; RSSC: Range Stack straw-tube tracking chambers; BVL: barrel-veto-liner photon counter; UPV: upstream photon-veto counter; AD: active degrader. Source: Figures taken from Refs.[57, 59].

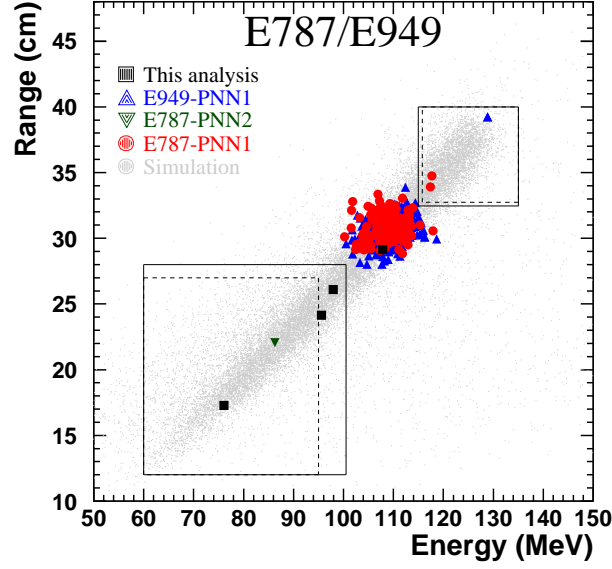


Figure 9: E949/E787 result on $K^+ \rightarrow \pi^+ \nu \bar{\nu}$: π^+ kinetic energy versus range plot of all events passing all other selection criteria. The solid (dashed) lines represent the limits of the PNN1/PNN2 signal regions for the E949 (E787) analyses. The light gray points are simulated $K^+ \rightarrow \pi^+ \nu \bar{\nu}$ events that were accepted by the trigger. Source: Figure taken from Ref.[59].

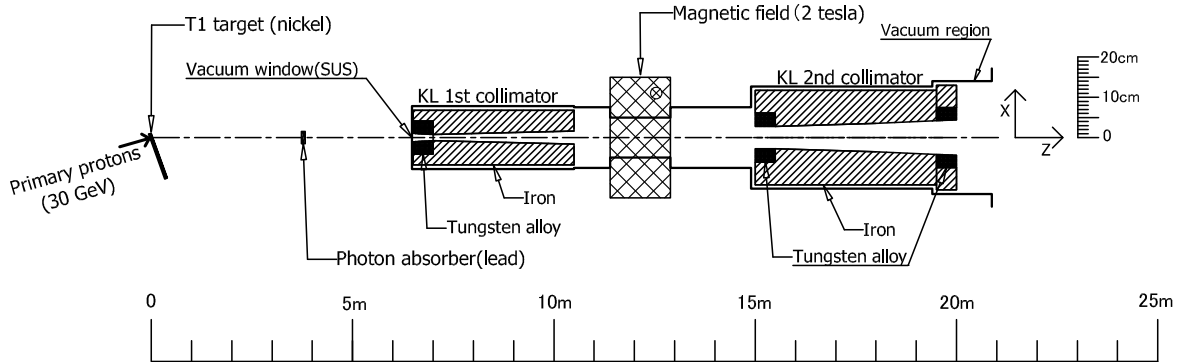


Figure 10: Schematic plan view of the neutral beam line for K^0 TO . Source: Figure taken from Ref.[66].

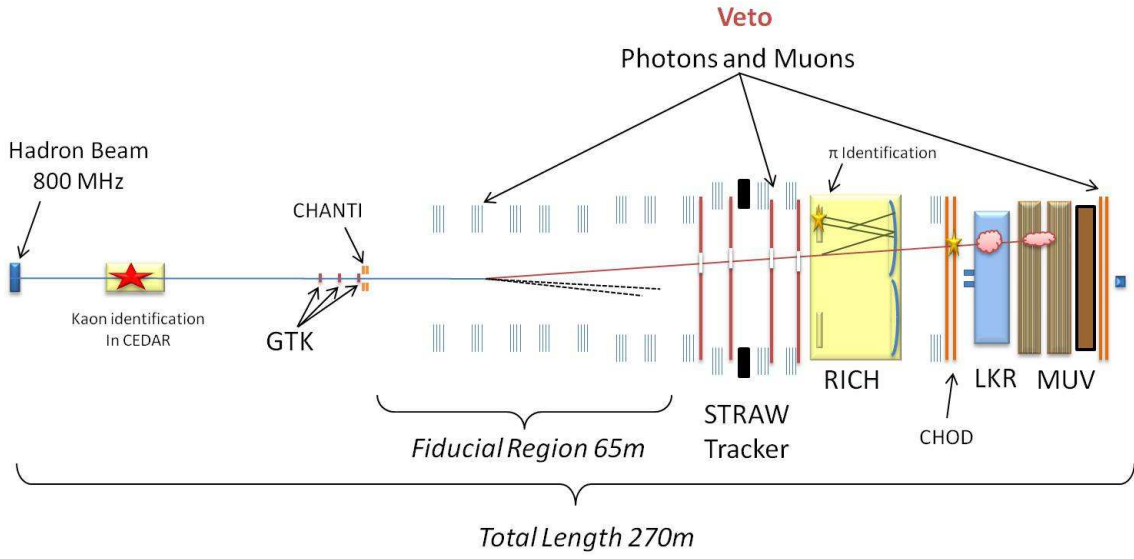


Figure 11: Schematic view of the NA62 beam line and detector. CEDAR: differential Čerenkov counter; GTK: silicon pixel tracking detectors; CHANTI: guard-ring counters; RICH: Ring-Imaging Čerenkov detector; CHOD: charged-particle hodoscope; LKR: liquid-Krypton calorimeter; MUV: muon-veto detectors. Source: Figure taken from Ref.[72].

3.3 $K \rightarrow \ell\bar{\ell}$ and $K \rightarrow \pi\ell\bar{\ell}$

Rare kaon decays with charged leptons should be easier to detect in experiments because the kaon mass can be fully-reconstructed. However, if a kaon decay accompanies charged leptons in the final state, the transition is also induced by long-distance effects with photon emission in hadronic interactions (Section 6); their theoretical interpretations are not straightforward. The decays $K_L^0 \rightarrow \mu^+\mu^-$ and $K_L^0 \rightarrow e^+e^-$ are measured to be $B(K_L^0 \rightarrow \mu^+\mu^-) = (6.84 \pm 0.11) \times 10^{-9}$ and $B(K_L^0 \rightarrow e^+e^-) = (9_{-4}^{+6}) \times 10^{-12}$, respectively [77]; the latter is the smallest branching ratio yet measured in particle physics. However, these decay modes are saturated by an absorptive process [78]: $K_L^0 \rightarrow \gamma\gamma$ and the two photons subsequently scattered into two leptons. We basically look at a QED process, and cannot get good information on the short distance contributions [79].

The KLOE experiment (to be discussed in Sections 4.3 and 5) obtained an upper limit of 9×10^{-9} [80] for the branching ratio of the $K_S^0 \rightarrow e^+e^-$ decay.

To the $K_L^0 \rightarrow \pi^0\ell\bar{\ell}$ decay, there are four contributions ⁸ from direct CP violation, indirect CP violation due to the K_1 component of K_L^0 (ICPV), their interference (INT), and the CP conserving process (CPC) through the $\pi^0\gamma^*\gamma^*$ intermediate state. The CPC contribution can be obtained from the study of the decay $K_L^0 \rightarrow \pi^0\gamma\gamma$ [84, 85]. The $K_S^0 \rightarrow \pi^0\ell\bar{\ell}$ decay, which is a CP conserving process of K_S^0 , helps to do reliable estimation of ICPV (and INT) and extract short-distance physics from $K_L^0 \rightarrow \pi^0\ell\bar{\ell}$ [81, 82]. New Physics impacts on the $K_L^0 \rightarrow \pi^0\ell\bar{\ell}$ decays are discussed in [83, 86].

The NA48/1 collaboration at CERN performed the data taking dedicated to K_S^0 decays with a high-intensity K_S^0 beam: 2×10^5 K_S^0 decays per spill with a mean energy of 120 GeV. The rare decays $K_S^0 \rightarrow \pi^0e^+e^-$ and $K_S^0 \rightarrow \pi^0\mu^+\mu^-$ were observed for the first time; using a vector matrix element and unit form factor, the measured branching ratios were $(5.8_{-2.3}^{+2.8}(\text{stat.}) \pm 0.8(\text{syst.})) \times 10^{-9}$ [87] and $(2.9_{-1.2}^{+1.5}(\text{stat.}) \pm 0.2(\text{syst.})) \times 10^{-9}$ [88], respectively. With these results and theoretical analyses, $B(K_L^0 \rightarrow \pi^0e^+e^-) = 3.23_{-0.79}^{+0.91} \times 10^{-11}$ and $B(K_L^0 \rightarrow \pi^0\mu^+\mu^-) = 1.29_{-0.23}^{+0.24} \times 10^{-11}$ with $a_S > 0$ and $B(K_L^0 \rightarrow \pi^0e^+e^-) = 1.37_{-0.43}^{+0.55} \times 10^{-11}$ and $B(K_L^0 \rightarrow \pi^0\mu^+\mu^-) = 0.86_{-0.17}^{+0.18} \times 10^{-11}$ with $a_S < 0$ are predicted in the SM [83], where a_S is a parameter of the form factors in the $K_S^0 \rightarrow \pi^0\ell\bar{\ell}$ amplitude.

The $K_L^0 \rightarrow \pi^0e^+e^-$ decay has been studied by the KTeV experiment. The limiting background was from the radiative Dalitz decay $K_L^0 \rightarrow e^+e^-\gamma\gamma$ ($B = (5.95 \pm 0.33) \times 10^{-7}$ [77]) with invariant mass of the two photons consistent with the nominal mass of π^0 [89]. Phase space cuts, which were applied to the data to suppress the background, reduced the signal acceptance by 25%. The number of events observed in the signal region was consistent with the expected background for both of their 1997 and 1999 data sets. Combining these results, the KTeV final result was $B(K_L^0 \rightarrow \pi^0e^+e^-) < 2.8 \times 10^{-10}$ [90]. KTeV also studied the $K_L^0 \rightarrow \pi^0\mu^+\mu^-$ decay, and has reported an upper limit $B(K_L^0 \rightarrow \pi^0\mu^+\mu^-) < 3.8 \times 10^{-10}$ [91] from the 1997 data set. Both of the limits are still an order of magnitude larger than the SM predictions.

The NA48/2 experiment measured the branching ratios of the $K^\pm \rightarrow \pi^\pm e^+e^-$ and $K^\pm \rightarrow \pi^\pm \mu^+\mu^-$ decays to be $(3.11 \pm 0.12) \times 10^{-7}$ [29] and $(9.62 \pm 0.25) \times 10^{-8}$ [30], respectively. The rates of these decays are dominated by the long-distance contributions involving one photon exchange, but the samples allow detailed studies of the decay properties such as the charge asymmetries (Section 2.2).

No new plan for the $K \rightarrow \ell\bar{\ell}$ and $K \rightarrow \pi\ell\bar{\ell}$ experiments is being proposed. The NA62 experiment is expected to collect samples of $K^+ \rightarrow \pi^+e^+e^-$ and $K^+ \rightarrow \pi^+\mu^+\mu^-$ decays which will be significantly larger than the current world samples.

⁸ Here we follow the discussions in [81, 82, 83] and use the convention of *direct* and *indirect* CP violation. As in $K_L^0 \rightarrow \pi^0\nu\bar{\nu}$, *direct* CP violation in $K_L^0 \rightarrow \pi^0\ell^+\ell^-$ corresponds to *interference between decays with and without mixing*.

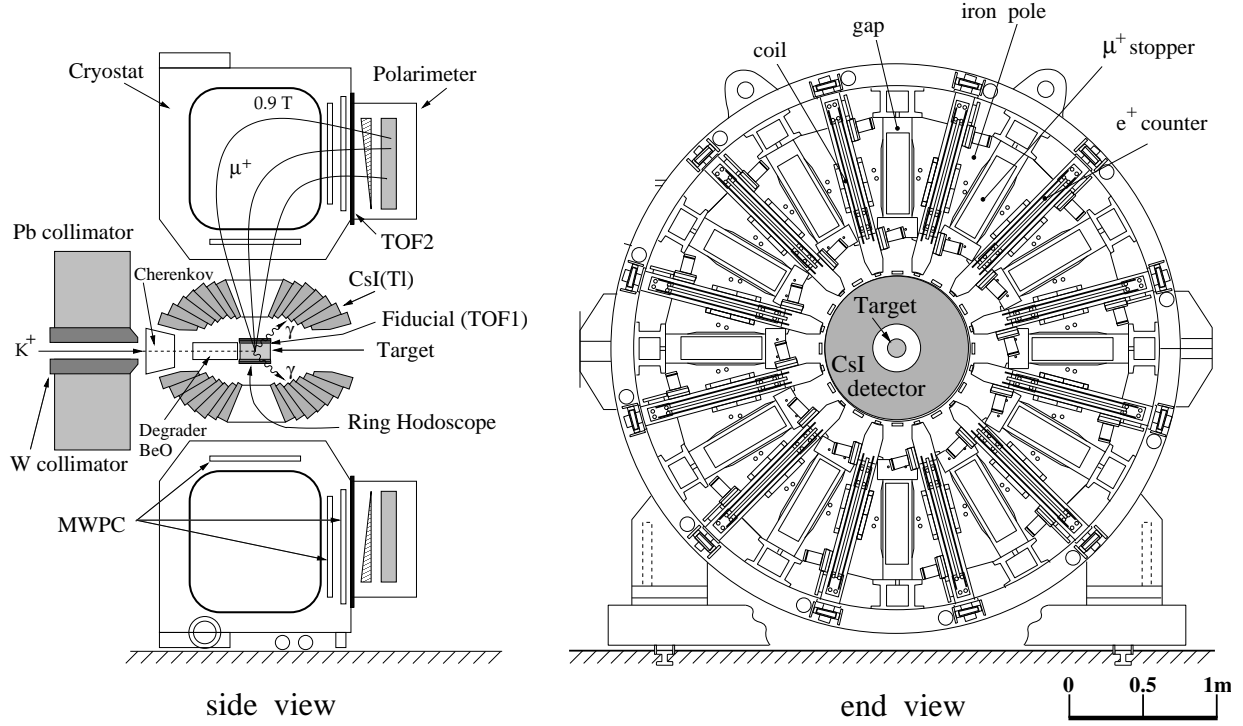


Figure 12: General assembly side and end views of the E246 detector. MWPC: multiwire proportional chamber for charged-particle tracking; TOF: time-of-flight counters for particle identification; CsI(Tl): thallium-doped CsI crystals to detect two photons from π^0 decay. Source: Figures taken from Ref.[94].

4 Leptons in kaon decays

This section covers the searches for explicit SM violations by measuring leptons in the final state of kaon decays.

4.1 Transverse muon polarization

In the $K^+ \rightarrow \pi^0 \mu^+ \nu$ decay ($K_{\mu 3}^+$, $B = (3.353 \pm 0.034)\%$ [77]), the transverse muon polarization p_t (the perpendicular component of the muon spin vector relative to the decay plane determined by the momentum vectors of muon and pion in the K^+ rest frame) is a T-odd quantity and is an observable of CP violation. Any spurious effect from final-state interactions is small ($< 10^{-5}$), because no charged particle other than muon exists in the final state. p_t is almost vanishing ($\sim 10^{-7}$) [92] in the SM, while new sources of CP violation (e.g. due to interference between the charged-Higgs exchange and the W exchange amplitudes) may give rise to p_t as large as 10^{-3} [93, 92]. Thus the transverse muon polarization in $K_{\mu 3}^+$ has been regarded as a sensitive probe of non-SM CP violation, and is a good example of looking beyond the SM by measuring a decay property with high statistics.

The E246 collaboration at KEK measured the charged track and photons from K^+ decays at rest. The E246 detector [94] is shown in Fig. 12. They used the superconducting toroidal spectrometer (consisting of 12 identical spectrometers arranged in rotational symmetry), which enabled the experiment to control possible sources of systematic uncertainties in polarization measurement. They accumulated 11.8M events and obtained $p_t = (-0.17 \pm 0.23(stat.) \pm 0.11(syst.)) \times 10^{-2}$ [95] by the total data sets of

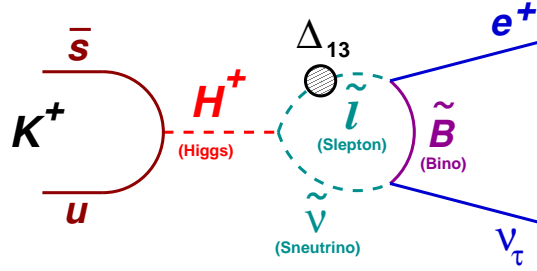


Figure 13: Diagram for the $K^+ \rightarrow e^+ \nu_\tau$ decay due to a new process induced by a charged-Higgs particle and an LFV loop of Supersymmetric particles. Δ_{13} represents the effective e - τ coupling constant in the loop. Source: Figure by courtesy of the NA62 collaboration.

E246 from 1996 to 2000, giving an upper limit $|p_t| < 0.0050$. They also performed the first measurement of p_t in the decay $K^+ \rightarrow \mu^+ \nu \gamma$: $p_t = (-0.64 \pm 1.85(stat.) \pm 0.10(syst.)) \times 10^{-2}$ [96].

A successor to E246 is another new kaon experiment at J-PARC, E06 TREK [97, 98], aiming at a p_t sensitivity of 10^{-4} . The E246 superconducting toroidal magnet will be used, and the detector will be upgraded by introducing the Gas Electron Multiplier (GEM) tracker and the active muon-polarimeter. A low-momentum beam line named K1.1BR was built at the Hadron Experimental Hall and was successfully commissioned in 2010.

4.2 Lepton flavor violation

Experimental search for lepton-flavor violating (LFV) kaon decays $K \rightarrow \mu e$ and $K \rightarrow \pi \mu e$ has a long history. The kaon system is well suited to the investigation of LFV new processes involving both quarks and charged leptons⁹ due to the high sensitivity achieved by experiments on this system. The mass of a hypothetical gauge boson for the tree-level effects should be in the scale of a few hundred TeV/ c^2 [99, 100]. A drawback is that the LFV processes induced by Supersymmetric loop effects are not so promising, because “Super-GIM” suppression mechanism is expected in both quark and lepton sectors [101].

Both two-body and three-body decays have to be explored in spite of the phase-space difference, because the $K \rightarrow \pi \mu e$ decay is sensitive to vector and scalar interactions. The upper limits on the $K_L^0 \rightarrow \mu^\pm e^\mp$ and $K^+ \rightarrow \pi^+ \mu^+ e^-$ branching ratios are 4.7×10^{-12} and 1.3×10^{-11} , respectively¹⁰ [77, 103]. The KTeV experiment set the upper limits for the branching ratios $B(K_L^0 \rightarrow \pi^0 \mu^\pm e^\mp) < 7.6 \times 10^{-11}$ and $B(K_L^0 \rightarrow \pi^0 \pi^0 \mu^\pm e^\mp) < 1.7 \times 10^{-10}$ in [104].

No new plan for the search for LFV kaon decays is being proposed.

4.3 Lepton flavor universality

The LFV kaon decays are currently studied, intensively, in the context of high precision tests of lepton flavor universality in the purely leptonic charged-kaon decay. The ratio $R_K \equiv \Gamma(K^+ \rightarrow e^+ \nu(\gamma))/\Gamma(K^+ \rightarrow \mu^+ \nu(\gamma))$ is helicity suppressed in the SM due to the V-A couplings and is predicted to be $R_K^{SM} = (2.477 \pm 0.001) \times 10^{-5}$ [105], in which the radiative decay $K^+ \rightarrow e^+ \nu \gamma$ ($K_{e2\gamma}$) via internal bremsstrahlung is included. On the other hand, suppose an LFV new decay $K^+ \rightarrow e^+ \nu_\tau$

⁹ Assuming an additive quantum number for quarks and leptons in the same generation (“one” for down-quark and electron, “two” for strange-quark and muon, ...), the net number is conserved in the LFV kaon decays.

¹⁰ The limit 4.7×10^{-12} on $B(K_L^0 \rightarrow \mu^\pm e^\mp)$ had been the most stringent upper limit to particle decays, until the MEG collaboration recently published an upper limit of 2.4×10^{-12} on the $\mu^+ \rightarrow e^+ \gamma$ branching ratio [102].

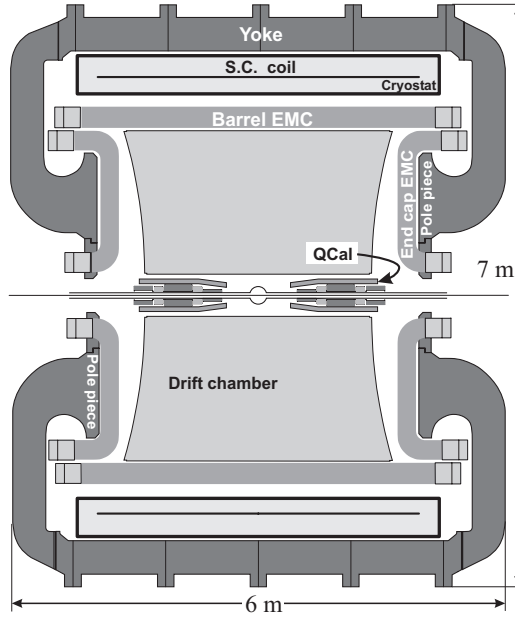


Figure 14: Vertical cross-section of the KLOE detector. QCal: lead/scintillator-tile calorimeters to detect photons that would be otherwise absorbed on the permanent quadrupole magnets for beam focusing; EMC: electromagnetic calorimeter; S.C. coil: superconducting coil. Source: Figure taken from Ref.[112].

exists due to the process of an intermediate charged-Higgs particle and an LFV Supersymmetric loop (Fig. 13) [106]. Since the neutrino flavor is undetermined experimentally, the measured R_K should be regarded as

$$R_K = \frac{\sum_i \Gamma(K^+ \rightarrow e^+ \nu_i)}{\sum_i \Gamma(K^+ \rightarrow \mu^+ \nu_i)} \simeq \frac{\Gamma_{SM}(K^+ \rightarrow e^+ \nu_e) + \Gamma_{NP}(K^+ \rightarrow e^+ \nu_\tau)}{\Gamma_{SM}(K^+ \rightarrow \mu^+ \nu_\mu)} \quad (7)$$

assuming that $\Gamma_{NP}(K^+ \rightarrow e^+ \nu_\mu)$ is small. The deviations from the SM prediction, denoted as ΔR_K , in the relative size of $10^{-2} \sim 10^{-3}$ are suggested [107]. In such a case, with the charged Higgs mass m_{H^+} , the ratio of the Higgs vacuum expectation values for the up- and down- quark masses (denoted as $\tan \beta$), and the effective $e - \tau$ coupling constant Δ_{13} , the size of ΔR_K is predicted as

$$\frac{\Delta R_K}{R_K^{SM}} = \frac{\Gamma_{NP}(K^+ \rightarrow e^+ \nu_\tau)}{\Gamma_{SM}(K^+ \rightarrow e^+ \nu_e)} = \left(\frac{m_{K^+}}{m_{H^+}} \right)^4 \left(\frac{m_\tau}{m_e} \right)^2 |\Delta_{13}|^2 \tan^6 \beta \quad (8)$$

and can be experimentally studied. The lepton flavor universality is also pursued by the PIENU experiment [108] at TRIUMF and the PEN experiment [109] at PSI to measure $\Gamma(\pi^+ \rightarrow e^+ \nu(\gamma))/\Gamma(\pi^+ \rightarrow \mu^+ \nu(\gamma))$ precisely.

The KLOE collaboration at DAΦNE, the Frascati ϕ factory [110, 111, 112], measured R_K with a data set consisting of 2.2 fb^{-1} collected during 2001-2005 [113], corresponding to 3.3 G $K^+ K^-$ pairs produced from ϕ meson decays. DAΦNE is an $e^+ e^-$ collider operated at a total energy $\sqrt{s} = m_\phi \cdot c^2 \sim 1.02 \text{ GeV}$. ϕ mesons were produced with a cross section of $\sim 3.1 \text{ } \mu\text{b}$ and decayed into $K^+ K^-$ pairs and $K_L^0 K_S^0$ pairs with branching ratios of 49% and 34%, respectively; thus, DAΦNE is a copious source of *tagged* and *monochromatic* kaons. The KLOE detector (Fig. 14), whose radius was 3.5 m to catch 63% of all decaying K_L^0 's, consisted of the cylindrical drift chamber and electromagnetic calorimeters with an axial magnetic field of 0.52 T. The $K^\pm \rightarrow \ell^\pm \nu$ decay in flight ($\sim 0.1 \text{ GeV}/c$) was reconstructed by the tracks

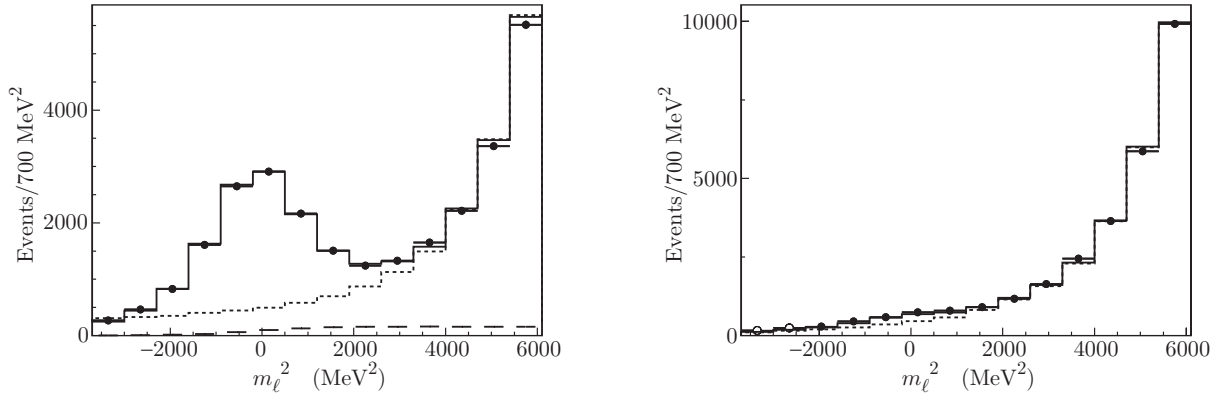


Figure 15: KLOE's $K^\pm \rightarrow e^\pm \nu$ analysis with the neural net output NN : the sum of fit results for K^+ and K^- projected onto the m_ℓ^2 axis in a signal region ($NN > 0.98$, left) and a background region ($0.86 < NN < 0.98$, right), for data (black dots), Monte Carlo fit (solid line), and $K_{\mu 2}$ background (dotted line). The contribution from K_{e2} events with $E_\gamma > 10$ MeV is shown in dashed line. Source: Figures taken from Ref.[113].

of a kaon and a decay product, with the same charge, in the drift chamber, and the squared mass m_ℓ^2 of the lepton for the decay :

$$m_\ell^2 = (E_K - |\vec{p}_K - \vec{p}_d|)^2 - (\vec{p}_d)^2 \quad (9)$$

was computed from the measured kaon and decay-particle momenta \vec{p}_K and \vec{p}_d . In the analysis, the $K^\pm \rightarrow e^\pm \nu$ events at around $m_\ell^2 = 0$ should be distinguished from the background contamination due to the tail of the prominent $K^\pm \rightarrow \mu^\pm \nu$ peak; the kinematic and track quality cuts were imposed and then the information about shower profile and total energy deposition in the calorimeter, combined with a neural network technique, and the time-of-flight information were used for electron identification (Fig. 15). The numbers of $K \rightarrow e\nu(\gamma)$ events were 7064 ± 102 for K^+ and 6750 ± 101 for K^- , respectively, 89.8% of which had $E_\gamma < 10$ MeV and contained both the $K \rightarrow e\nu$ events and the $K_{e2\gamma}$ events with $E_\gamma < 10$ MeV. No photon detection requirement was imposed; the contribution from the $K_{e2\gamma}$ events with $E_\gamma > 10$ MeV, due to the direct-emission process, was studied [113, 114] by using a separate sample with photon detection requirement, and was subtracted. The numbers of $K \rightarrow \mu\nu(\gamma)$ events were 287.8M for K^+ and 274.2M for K^- , respectively. The difference between the K^+ and K^- counts was due to the larger cross section of K^- nuclear interaction in the material traversed. Finally, KLOE obtained $^{11} R_K = (2.493 \pm 0.025(stat.) \pm 0.019(syst.)) \times 10^{-5}$, in agreement with the SM prediction.

The NA62 collaboration at CERN, in the first phase, collected data to measure R_K during four months in 2007, and collected special data samples to study systematic effects for two weeks in 2008. The beam line and setup of NA48/2 were used; 90% of the data were taken with the un-separated K^+ beam of $74.0 \pm 1.4(\text{rms})$ GeV/c, because the muon sweeping system optimized for the positive beam provided better suppression of the positrons produced by beam halo muons via $\mu \rightarrow e$ decay. The LKr calorimeter was used for lepton identification as well as a photon veto with the energy threshold of 2 GeV. Results based on the analysis of 40% of the 2007 data collected with the K^+ beam only were published in [115]. The kinematic identification of $K^+ \rightarrow \ell^+ \nu$ decays is based on the reconstructed squared missing-mass $M_{miss}^2(\ell)$ in the positron ($\ell = e$) or muon ($\ell = \mu$) hypothesis:

$$M_{miss}^2 = (P_K - P_\ell)^2 \quad (10)$$

¹¹ The rate R_{10} , defined as $R_{10} = \Gamma(K \rightarrow e\nu(\gamma), E_\gamma < 10 \text{ MeV})/\Gamma(K \rightarrow \mu\nu)$, was measured and was converted into R_K with the relation $R_{10} = R_K \times (0.9357 \pm 0.0007)$.

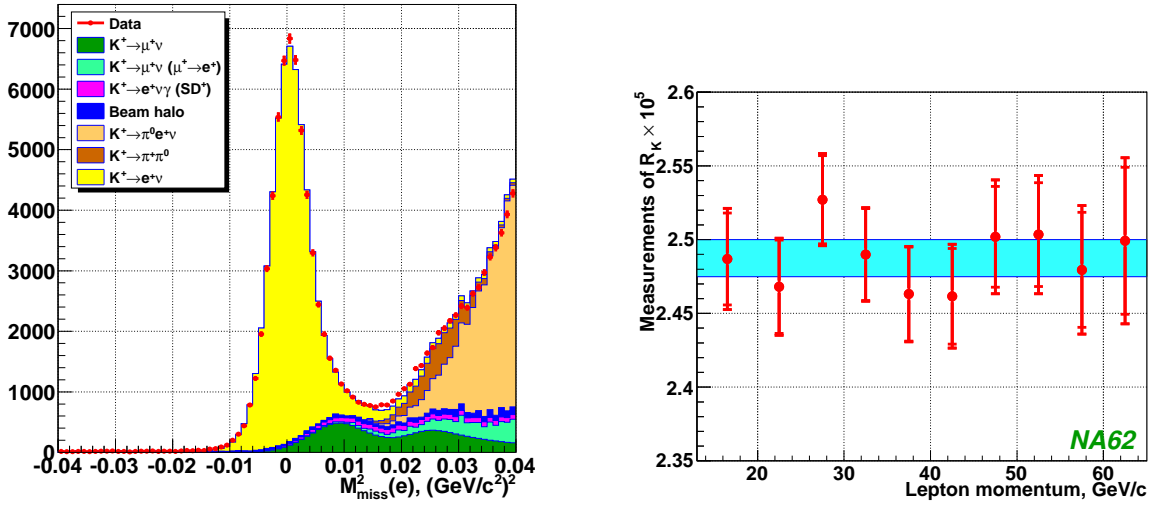


Figure 16: NA62’s $K^\pm \rightarrow e^\pm \nu$ analysis: reconstructed squared missing-mass $M_{miss}^2(e)$ distribution of the $K^+ \rightarrow e^+ \nu$ candidates compared with the sum of normalized estimated signal and background components (left); measurements of R_K in lepton momentum bins, with the average R_K and its total uncertainty indicated by a band (right). Source: Figures taken from Ref. [115].

from the average kaon four-momentum P_K (monitored in time with $K^+ \rightarrow \pi^+ \pi^+ \pi^-$ decays) and the reconstructed lepton four-momentum P_ℓ under the positron or muon mass hypothesis (Fig. 16 left). The number of reconstructed $K^+ \rightarrow e^+ \nu$ candidate events was 59813, and the number of $K^+ \rightarrow \mu^+ \nu$ candidate events was 18.03M. The total background contamination was $(8.71 \pm 0.24) \%$; the main source of the background was found to be the $K^+ \rightarrow \mu^+ \nu$ decay with muon identification as positron due to *catastrophic* bremsstrahlung in or in front of the LKr calorimeter. The probability of the misidentification was studied with pure muon samples, without positron contamination (typically $\sim 10^{-4}$) due to $\mu^+ \rightarrow e^+$ decays in flight. The sample was selected from the tracks traversing a $9.2X_0$ -thick lead wall, covering 20% of the geometrical acceptance, which was installed 1.2 m in front of the LKr calorimeter during a dedicated period. The $K^+ \rightarrow \mu^+ \nu$ background contamination was estimated to be $(6.11 \pm 0.22) \%$. Due to the significant dependence of acceptance and background on lepton momentum, the R_K measurement was performed independently in ten momentum bin covering a range from 13 to 65 GeV/c (Fig. 16 right). The selection criteria had been optimized separately in each momentum bin. R_K was obtained to be $(2.487 \pm 0.011(stat.) \pm 0.007(syst.)) \times 10^{-5}$, consistent with the SM prediction.

The NA62 collaboration recently reported results based on the analysis of the full data set [116], superseding the results in [115]. They obtained $R_K = (2.488 \pm 0.007(stat.) \pm 0.007(syst.)) \times 10^{-5}$ and, combining with other R_K measurements, the world average is $(2.488 \pm 0.009) \times 10^{-5}$, with 0.4% precision, as presented in Fig. 17 left. The regions excluded at 95% C.L. in the $(M_{H^+}, \tan \beta)$ plane are shown in Fig. 17 right, for different values of Δ_{13} .

The R_K measurement will continue in the next phase of NA62 for $K^+ \rightarrow \pi^+ \nu \bar{\nu}$ as well as in the future KLOE-2 experiment (Section 5). The TREK collaboration at J-PARC has also submitted a proposal P36 [117], as their first phase, to measure R_K with K^+ decays at rest.

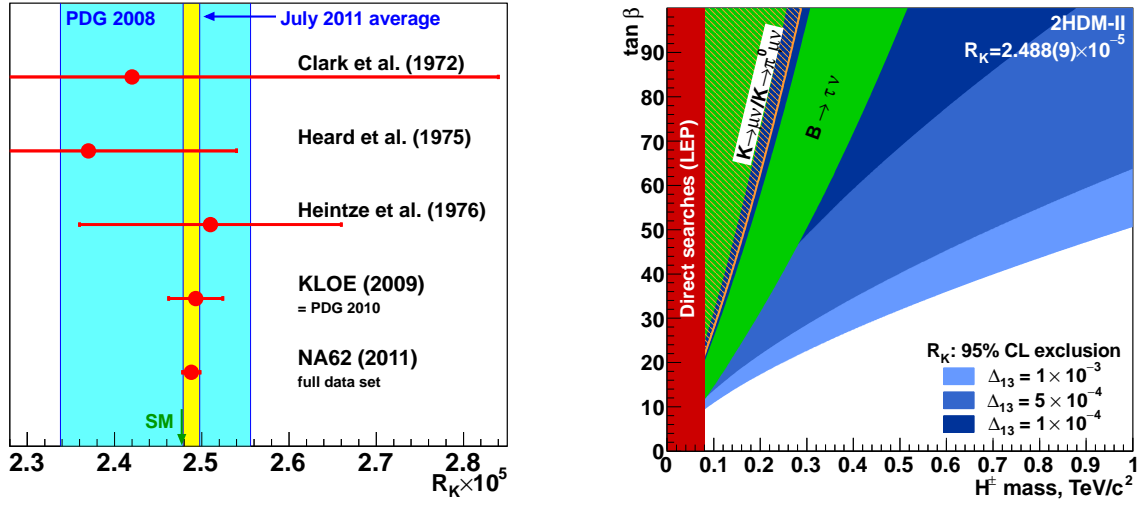


Figure 17: Summary of the R_K measurements including NA62's new results in [116] (left); excluded regions at 95% C.L. in the $(m_{H^+}, \tan \beta)$ plane for $\Delta_{13} = 10^{-4}$, 5×10^{-4} and 10^{-3} with the constraints from other experiments (right). Source: Figures by courtesy of the NA62 collaboration.

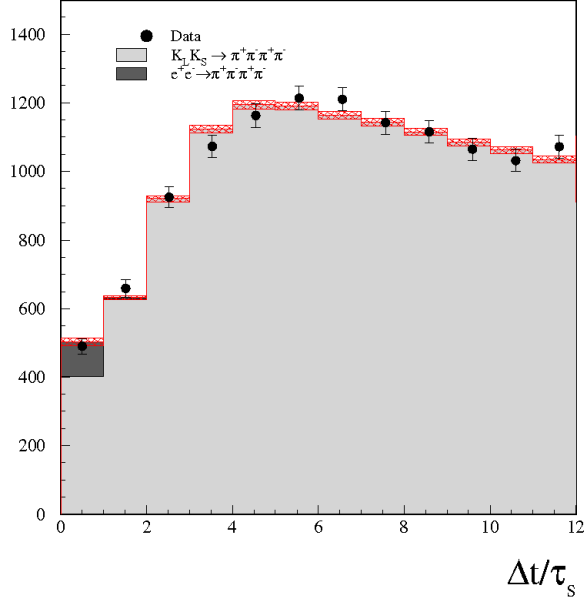


Figure 18: KLOE result on the fit to the measured $I(\Delta t)$ distribution of $\phi \rightarrow K_S^0 K_L^0 \rightarrow \pi^+ \pi^- \pi^+ \pi^-$. The black points with errors are data and the solid histogram is the fit result. The uncertainty arising from the efficiency correction is shown as the hatched area. Source: Figure taken from Ref.[121].

5 Tests of CPT and quantum mechanics

In the ϕ decay into $K_L^0 K_S^0$ pairs, the initial state is a coherent (and entangled) quantum state:

$$|i\rangle = \frac{1}{\sqrt{2}} [|K^0\rangle |\bar{K}^0\rangle - |\bar{K}^0\rangle |K^0\rangle] = \frac{N}{\sqrt{2}} [|K_S^0\rangle |K_L^0\rangle - |K_L^0\rangle |K_S^0\rangle] \quad (11)$$

where $N \simeq 1$ is a normalization factor. In the KLOE experiment, by tagging the events with K_L^0 reaching the calorimeter without decaying (dubbed “K-crash”), a pure K_S^0 beam was available and there has been a major improvement in K_S^0 decay measurements (to be discussed in Section 8). With the results of various new measurements on neutral kaon decays, the Bell-Steinberger relation was used [118] to provide a constraint relating the unitarity of the sum of the decay amplitudes to the CPT observables. The latest limit on the mass difference between K^0 and \bar{K}^0 was 4.0×10^{-19} GeV at the 95% C.L. [119].

In the CP-violating process $\phi \rightarrow K_S^0 K_L^0 \rightarrow \pi^+ \pi^- \pi^+ \pi^-$, KLOE observed the quantum interference between two kaons for the first time [120]. The measured Δt distribution, with Δt the absolute value of the time difference of the two $\pi^+ \pi^-$ decays, can be fitted with the distribution in the $K_S^0 - K_L^0$ basis:

$$I(\Delta t) \propto e^{-\Gamma_L \Delta t} + e^{-\Gamma_S \Delta t} - 2(1 - \zeta_{SL}) e^{-\frac{(\Gamma_S + \Gamma_L)}{2} \Delta t} \cos(\Delta m \Delta t) \quad (12)$$

$$\rightarrow 2\zeta_{SL} \left(1 - \frac{(\Gamma_S + \Gamma_L)}{2} \Delta t \right) \quad \Delta t \rightarrow 0 \quad (13)$$

where Δm is the mass difference between K_L^0 and K_S^0 . The interference term $e^{-\frac{(\Gamma_S + \Gamma_L)}{2} \Delta t} \cos(\Delta m \Delta t)$ is multiplied by a factor $(1 - \zeta_{SL})$ with a *decoherence* parameter ζ_{SL} , which represents a loss of coherence

during the time evolution of the states and should be zero in quantum mechanics (QM). Final results obtained from KLOE with 1.5 fb^{-1} in 2004-2005 were [121] $\zeta_{SL} = (0.3 \pm 1.8(\text{stat.}) \pm 0.6(\text{syst.})) \times 10^{-2}$ (Fig. 18) and, to the fit with the distribution in the $K^0 - \bar{K}^0$ basis, $\zeta_{0\bar{0}} = (1.4 \pm 9.5(\text{stat.}) \pm 3.8(\text{syst.})) \times 10^{-7}$; no deviation from QM was observed ¹². Since the measurement of non-zero ζ_{SL} is sensitive to the distribution in the small Δt region, the decay vertex resolution due to charged-track extrapolation ($\simeq 6 \text{ mm}$ in the KLOE detector, corresponding to $\sim 1\tau_S$, to the vertex of a $K_S^0 \rightarrow \pi^+\pi^-$ decay close to the interaction point) should be improved in future experiments. Other tests of CPT invariance and the basic principles of QM are discussed in [121, 122].

Kaon physics at the ϕ factory will continue with an upgraded KLOE detector, KLOE-2 [123, 124]. In 2008, DAΦNE was upgraded with a new interaction scheme (*Crabbed Waist* collisions [125]). During 2008-2009 a factor-of-three larger peak-luminosity ($4.53 \times 10^{32} \text{ cm}^{-2}\text{s}^{-1}$) and a factor-of-two larger integrated luminosity per an hour (1 pb^{-1}) than what previously obtained were achieved [126]. The DAΦNE commissioning is scheduled to be resumed in October 2011. In the first phase, the detector with minimal upgrade (two devices along the beam line to tag the scattered electrons/positrons from $\gamma\gamma$ collisions) restarts taking data. To the next phase, a cylindrical GEM detector [127] will be placed between the beam pipe and the inner wall of the drift chamber, as a new Inner Tracker, to improve the decay vertex resolution and to increase the acceptance for low transverse-momentum tracks. A crystal calorimeter with timing (CCALT) for low-angle and low-energy photons and a quadrupole calorimeter with tiles (QCALT) to cover the area of the final focusing section will also be installed. From 2013 to 2015, physics run to integrate 20 fb^{-1} with the KLOE-2 detector is expected [128, 129].

¹² Decoherence in the $K^0 - \bar{K}^0$ basis results in the CP-allowed $K_S^0 K_S^0 \rightarrow \pi^+\pi^-\pi^+\pi^-$ decays and thus the value for the decoherence parameter $\zeta_{0\bar{0}}$ is much smaller than ζ_{SL} .

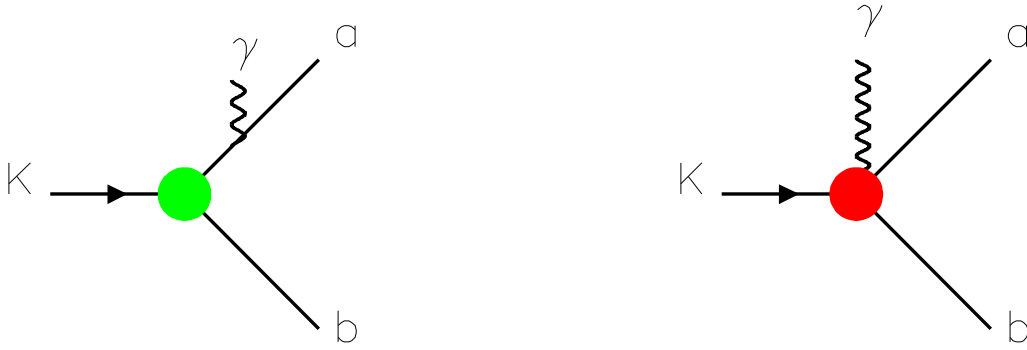


Figure 19: Graphs of the IB (left) and SD or DE (right) components of the radiative $K \rightarrow ab$ decay.

6 Radiative decays

A *radiative* kaon decay, which is accompanied by real photons in the final state, is due to radiative effects in the leptonic, semileptonic, or non-leptonic transitions. The decay can proceed via

- inner bremsstrahlung (IB), in which a photon is emitted from the charged particle in the initial or final state (Fig. 19 left),
- structure-dependent (SD) or direct-emission (DE) radiative decay¹³, which involves the emission of a photon from the intermediate states in the transition (Fig. 19 right), and
- their possible interference (INT).

Processes where a photon internally converts into an e^+e^- pair or a $\mu^+\mu^-$ pair (if kinematically allowed), called a Dalitz pair [130], can also be considered; the plane of the Dalitz pair in the kaon rest frame contains information on the polarization of the virtual photon.

Radiative kaon decays occur at the branching ratio of $10^{-3} \sim 10^{-8}$ and are categorized as “medium” decays. In general, the IB contribution dominates the decays, but the relative size is suppressed if the intrinsic decay, with which the photon is associated, is suppressed or forbidden (e.g. the $K_L^0 \rightarrow \pi^+\pi^-$ decay by CP symmetry and the $K^+ \rightarrow \pi^+\pi^0$ decay by the $\Delta I = 1/2$ rule). A better understanding of radiative decays, not only the branching ratios but also the decay spectra, is important (and occasionally crucial) to do rare decay search and precise measurement. The $K_L^0 \rightarrow \pi^0\gamma\gamma$ decay to the $K_L^0 \rightarrow \pi^0\ell\bar{\ell}$ predictions (Section 3.3) and the $K^\pm \rightarrow e^\pm\nu\gamma$ decay to the $K^\pm \rightarrow e^\pm\nu$ analysis (Section 4.3) are good examples.

The IB component of a decay is a QED radiative correction to the intrinsic decay and can be predicted reliably. On the other hand, the SD or DE component is essentially due to low-energy hadronic interactions, to which the effective-field approach based on chiral symmetry, chiral perturbation theory¹⁴ [135], is applicable. In the theory, the quark fields are represented instead by the pseudoscalar-

¹³ Traditionally, the emission in the leptonic or semileptonic transition is called structure dependent (because it is sensitive to the hadronic structure of kaon) and the emission in the non-leptonic transition is called direct emission (because it is due to hadronic interactions of mesons); however, not all the papers follow the convention.

¹⁴ The techniques using chiral symmetry, called *chiral dynamics*, were developed in the late 1960’s and yield the results to meson interactions derived earlier by *PCAC* and *current algebra*. However, there had been no framework to do systematic calculations of hadron decays in the energy region below 1 GeV. In 1979, Weinberg introduced the concept of effective field theories using effective Lagrangians and proposed the application to strong interactions [131, 132]. Gasser and Leutwyler, in 1984 and 1985, materialized Weinberg’s program and expanded the use of chiral Lagrangian to the higher order [133, 134]. This approach is called *chiral perturbation theory*, and has been intensively used in particle and nuclear physics as a theory of low energy QCD.

Table 3: Radiative kaon decays in the last five years [77].

mode	branching ratio	kinematic region*	new results from
$K_L^0 \rightarrow \pi^\pm e^\mp \nu_e \gamma$	$(3.79 \pm 0.06) \times 10^{-3}$	$E_\gamma > 30\text{MeV}, \theta_{e\gamma} > 20^\circ$	KLOE [137]
$K_L^0 \rightarrow \pi^\pm e^\mp \nu_e e^+ e^-$	$(1.26 \pm 0.04) \times 10^{-5}$	$M_{ee} > 5\text{MeV}, E_{ee} > 30\text{MeV}$	KTeV [138]
$K_L^0 \rightarrow \pi^0 \gamma \gamma$	$(1.273 \pm 0.034) \times 10^{-6}$		KTeV [85]
$K_L^0 \rightarrow \pi^0 \gamma e^+ e^-$	$(1.62 \pm 0.17) \times 10^{-8}$		KTeV [139]
$K_L^0 \rightarrow e^+ e^- \gamma$	$(9.4 \pm 0.4) \times 10^{-6}$		KTeV [140]
$K_S^0 \rightarrow \pi^+ \pi^- e^+ e^-$	$(4.79 \pm 0.15) \times 10^{-5}$		NA48/1 [141]
$K_S^0 \rightarrow \gamma \gamma$	$(2.63 \pm 0.17) \times 10^{-6}$		KLOE [142]
$K^+ \rightarrow e^+ \nu_e \gamma$	$(9.4 \pm 0.4) \times 10^{-6}$	$E_\gamma > 10\text{MeV}, p_e > 200\text{MeV}/c$	KLOE [113]
$K^+ \rightarrow \pi^0 e^+ \nu_e \gamma$	$(2.56 \pm 0.16) \times 10^{-4}$	$E_\gamma > 10\text{MeV}, 0.6 < \cos(\theta_{e\gamma}) < 0.9$	ISTRA+ [143]
$K^+ \rightarrow \pi^0 \mu^+ \nu_\mu \gamma$	$(1.25 \pm 0.25) \times 10^{-5}$	$30 < E_\gamma < 60\text{MeV}$	E787 [144]
			ISTRA+ [145]
$K^+ \rightarrow \pi^+ \pi^0 \gamma$ (INT)	$(-4.2 \pm 0.9) \times 10^{-6}$	$0 < T_{\pi^+} < 80\text{MeV}$	NA48/2 [31]
$K^+ \rightarrow \pi^+ \pi^0 \gamma$ (DE)	$(6.0 \pm 0.4) \times 10^{-6}$	$0 < T_{\pi^+} < 80\text{MeV}$	NA48/2 [31]
$K^+ \rightarrow \pi^+ e^+ e^- \gamma$	$(1.19 \pm 0.13) \times 10^{-8}$	$m_{ee\gamma} > 260\text{MeV}$	NA48/2 [146]

* Kinematic regions are defined in the kaon rest frame.

meson fields and the interactions are constructed based on chiral symmetry to the Nambu-Goldstone bosons. The Lagrangian \mathcal{L} is given in an expansion in powers of derivatives (∂_μ) to the fields, i.e. their external momenta (p), and with phenomenological coupling constants, and the interactions vanish in the limit $p \rightarrow 0$. By replacing the derivative in \mathcal{L} to the covariant derivative (D_μ), the electroweak interactions are introduced to the theory and decay diagrams involving kaons and pions can be calculated. Many applications to the medium kaon decays are collected in the DAΦNE Physics Handbook [136]. Since chiral perturbation theory is an effective field theory and does not make “perturbative” calculations (and convergence) in the usual sense of Quantum Field Theory, the theory should be verified by comparing the predictions with experiments, including the measurements of radiative kaon decays.

In table 3, radiative neutral- and charged-kaon decays whose new branching-ratio measurement was published in the last five years are listed. Some of them were measured as a byproduct of the experiment with the data collected by a pre-scaled physics or calibration trigger. It should be noted that, since the detector system has an energy threshold for photon detection and, also in the theoretical calculation, a cutoff to the photon energy is set in order to avoid infrared divergence to the IB component, a radiative decay is usually measured in a specific kinematic region.

The ISTRA+ collaboration at IHEP measured K^- decays in flight with the 26 GeV/ c un-separated secondary beam from U-70, the IHEP 70GeV proton synchrotron, in 2001. The ISTRA+ detector, with the spectrometer, lead-glass electromagnetic calorimeter (SP₁) and sampling hadron calorimeter (HC), is shown in Fig. 20. They reported the measurements of $K^- \rightarrow \pi^0 e^- \nu_e \gamma$ [143] and $K^- \rightarrow \pi^0 \mu^- \nu_\mu \gamma$ [145].

As a successor to ISTRA+, a new “OKA” experimental program [148] with RF-separated K^\pm beam is ongoing at U-70 of IHEP.

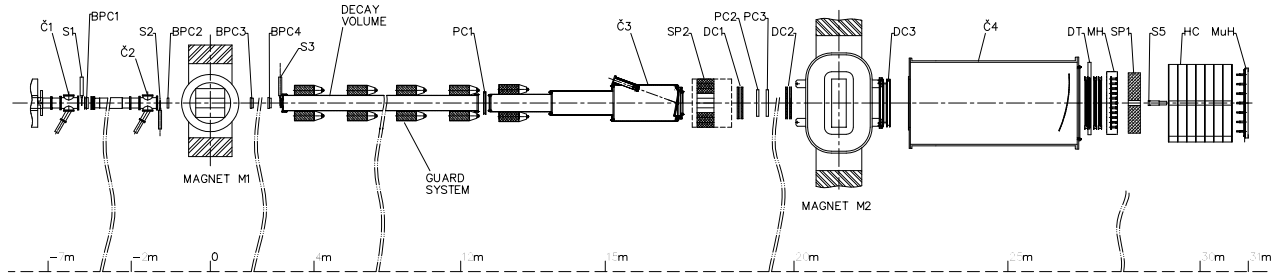


Figure 20: Elevation view of the ISTR+ detector. BPC1-BPC4: multiwire chambers for tracking beam particles; Č1 and Č2: threshold Čerenkov counters for kaon identification; S1-S3: scintillating counters for beam trigger, SP2: lead-glass calorimeter to detect large-angle photons, PC1-PC3, DC1-DC3, and DT: proportional chambers, drift chambers and drift tubes, respectively, for tracking decay products; Č3 and Č4: wide-aperture threshold Čerenkov counters; MH: scintillating hodoscope; SP1, HC, and MuH: lead-glass calorimeter, iron-scintillator sampling hadron calorimeter, and muon hodoscope, respectively, for decay products; S5: scintillating counter at the downstream of the setup to veto beam particles which do not decay. Source: Figure taken from Ref.[147].

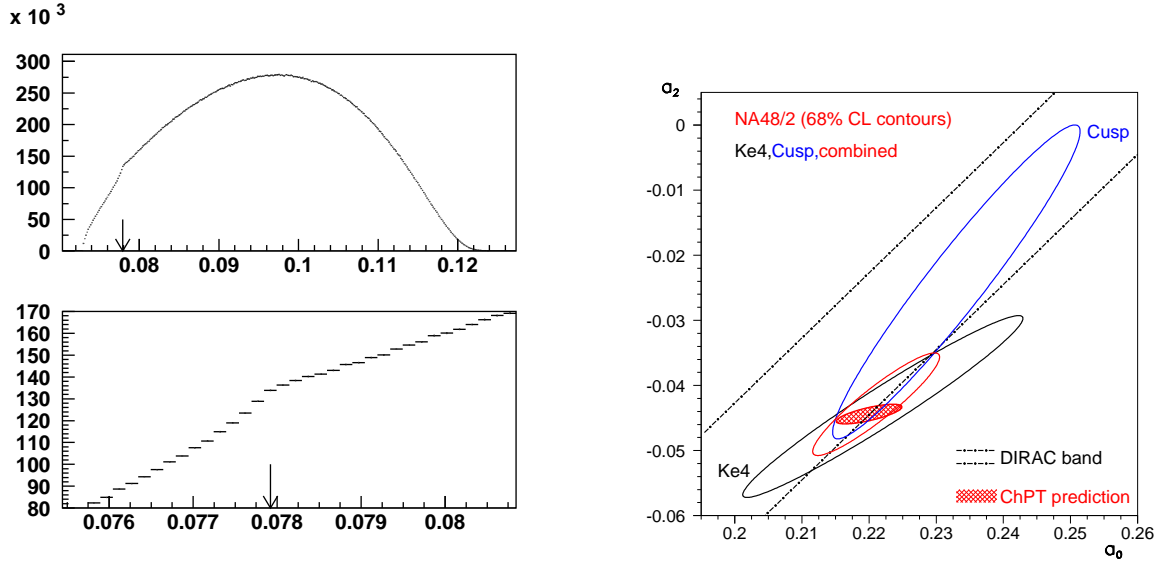


Figure 21: Cusp in $K^\pm \rightarrow \pi^\pm \pi^+ \pi^-$ by NA48/2: distribution of the square of the $\pi^0 \pi^0$ invariant mass, M_{00}^2 , in units of $(\text{GeV}/c^2)^2$ and enlargement of a narrow region around $M_{00}^2 = (2m_{\pi^+})^2$ (left); NA48/2 K_{e4} and cusp results from two-parameter fits in the (a_0, a_2) plane (right). In the right figure, the smallest contour corresponds to the combination of NA48/2 results, the cross-hatched ellipse is the prediction of chiral perturbation theory, and the dashed-dotted lines correspond to the recent results from the DIRAC experiment [151]. Source: Figures taken from Ref.[157] (left) and by courtesy of B. Bloch-Devaux (right).

7 Hadrons in kaon decays

As a theory of low energy QCD, the most reliable predictions of chiral perturbation theory are the S-wave $\pi\pi$ scattering lengths a_I in the isospin $I = 0$ and $I = 2$ states [149, 150]: $a_0 = 0.220 \pm 0.005$, $a_2 = -0.0444 \pm 0.0010$, and $(a_0 - a_2) = 0.264 \pm 0.004$ in units of $1/m_{\pi^+}$, where m_{π^+} is the charged-pion mass. The DIRAC collaboration at CERN produced $\pi^+ \pi^-$ atoms to measure its lifetime, and recently obtained $|a_0 - a_2| = 0.2533^{+0.0080}_{-0.0078}(\text{stat.})^{+0.0078}_{-0.0073}(\text{syst.})$ [151]. The $\pi\pi$ scattering lengths can also be determined by precise measurement of the kaon decays with two pions in the final state.

In the $\pi^0 \pi^0$ invariant-mass (M_{00}) distribution in the $K^\pm \rightarrow \pi^\pm \pi^0 \pi^0$ decay, the NA48/2 experiment observed a *cusp*-like anomaly in the region near $M_{00} = 2m_{\pi^+}$ (Fig. 21 left). The cusp was interpreted as an effect due to the interference of the two $K^\pm \rightarrow \pi^\pm \pi^0 \pi^0$ amplitudes; the first one is the intrinsic $K^\pm \rightarrow \pi^\pm \pi^0 \pi^0$ transition and the second one is $K^\pm \rightarrow \pi^\pm \pi^+ \pi^-$ followed by final state rescattering $\pi^+ \pi^- \rightarrow \pi^0 \pi^0$ [152, 153]. Fits to the M_{00} distribution from the 2003 and 2004 data sets using two formulations with several theoretical issues [154, 155, 156] taken into account, NA48/2 obtained the results from the cusp of $K^\pm \rightarrow \pi^\pm \pi^0 \pi^0$ as $(a_0 - a_2) = 0.2571 \pm 0.0048(\text{stat.}) \pm 0.0025(\text{syst.}) \pm 0.0014(\text{ext.})$ and $a_2 = -0.024 \pm 0.013(\text{stat.}) \pm 0.009(\text{syst.}) \pm 0.002(\text{ext.})$ [157].

The properties of the $K^\pm \rightarrow \pi^+ \pi^- e^\pm \nu$ (K_{e4}) decay, which has no other hadron than two pions in the final state, were measured by the NA48/2 experiment based on the statistics, 1.13M events from the 2003 and 2004 data sets, better than the previous experiments [158, 159]. As a result of the analysis, the difference (shift) δ between the S-wave, $I = 0$ and P-wave, $I = 1$ form-factor phases [160], δ_0^0 and δ_1^1 , was obtained as a function of the $\pi^+ \pi^-$ invariant mass. The phase shift $\delta = (\delta_0^0 - \delta_1^1)$ is related to the $\pi\pi$ scattering lengths by using numerical solutions [161, 162] of the Roy equations [163], which are a set of

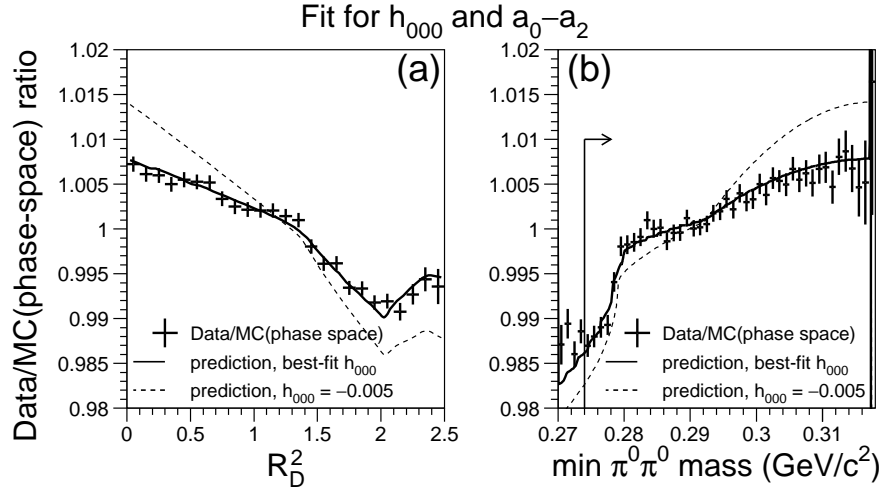


Figure 22: Cusp in $K_L^0 \rightarrow \pi^0 \pi^0 \pi^0$ by KTeV: distributions of the data/MC(phase-space) ratio as a function of R_D^2 (left) and the minimum $\pi^0 \pi^0$ mass (right). The solid curve is the prediction from the best fit, and the dashed curve is the prediction from the Dalitz-plot density with $h_{000} = -0.005$ without the rescattering effect. Source: Figures taken from Ref.[169].

dispersion relations for the partial wave amplitudes of $\pi\pi$ scattering. After taking the isospin-breaking effects [164] into account, NA48/2 obtained $a_0 = 0.2220 \pm 0.0128(stat.) \pm 0.0050(syst.) \pm 0.0037(th.)$ and $a_2 = -0.0432 \pm 0.0086(stat.) \pm 0.0034(syst.) \pm 0.0028(th.)$ [165] from the K_{e4} decay. Finally, combining both the K_{e4} and cusp results from NA48/2 (Fig. 21 right) without using the relation between a_0 and a_2 from chiral perturbation theory, $a_0 = 0.2210 \pm 0.0047(stat.) \pm 0.0040(syst.)$, $a_2 = -0.0429 \pm 0.0044(stat.) \pm 0.0028(syst.)$, and $(a_0 - a_2) = 0.2639 \pm 0.0020(stat.) \pm 0.0015(syst.)$ were obtained [165] as the most precise tests of low energy QCD from the kaon decay properties.

The Dalitz plot density of $K^\pm \rightarrow \pi^\pm \pi^0 \pi^0$ should be described with the known cusp in the region near $M_{00} = 2m_{\pi^+}$; the NA48/2 experiment proposed a new empirical model-independent parametrization of the $K^\pm \rightarrow \pi^\pm \pi^0 \pi^0$ Dalitz plot with seven parameters, and provided the values obtained by fitting their data [166]. Rescattering effects are much smaller in the $K^\pm \rightarrow \pi^\pm \pi^+ \pi^-$ decay¹⁵; the parametrization in Eq. (3) is still valid, and the NA48/2 experiment measured the values of the slope parameters [167]. NA48/2 also obtained, concurrently with their phase-shift measurements, the form factors in the matrix element of the K_{e4} decay [165, 168].

In the $K_L^0 \rightarrow \pi^0 \pi^0 \pi^0$ decay, the KTeV experiment also observed a cusp in the region where the minimum $\pi^0 \pi^0$ invariant-mass is near $2m_{\pi^+}$, though the cusp is smaller than in $K^\pm \rightarrow \pi^\pm \pi^+ \pi^-$ and is visible (Fig. 22) in the distribution of the ratio to the phase-space Monte Carlo (MC). The $K_L^0 \rightarrow \pi^0 \pi^0 \pi^0$ Dalitz-plot density is parametrized as

$$|M(R_D)|^2 \propto 1 + h_{000} \cdot R_D^2, \quad (14)$$

where the coefficients h_{000} is the quadratic slope parameter and R_D is the distance from the center of the Dalitz plot. Using the model in [153] and fitting the data for both h_{000} and $(a_0 - a_2)$ in a two-parameter fit, KTeV obtained $h_{000} = (-2.09 \pm 0.62(stat.) \pm 0.72(syst.) \pm 0.28(ext.)) \times 10^{-3}$ and $(a_0 - a_2) = 0.215 \pm 0.014(stat.) \pm 0.025(syst.) \pm 0.006(ext.)$ [169] from $K_L^0 \rightarrow \pi^0 \pi^0 \pi^0$.

¹⁵ Since the invariant mass of any two pion pair in $K^\pm \rightarrow \pi^\pm \pi^+ \pi^-$ is always $\geq 2m_{\pi^+}$, any cusp structure in the decay is outside the physical region.

New form factor measurements were reported by KLOE [170] on $K_L^0 \rightarrow \pi^\pm e^\mp \nu$ and by KTeV [171], KLOE [172] and NA48 [173] on $K_L^0 \rightarrow \pi^\pm \mu^\mp \nu$ as well as by KLOE [113] on $K^\pm \rightarrow e^\pm \nu \gamma$ and by ISTRA+ [147] on $K^- \rightarrow \mu^- \nu \gamma$.

Table 4: Kaon basic observables*.

observable	unit	value in PDG2010 [77]	value in PDG2000 [179]	new results from
K^0 mass: m_{K^0}	MeV/ c^2	497.614 ± 0.024	497.672 ± 0.031	KLOE, NA48
K_L^0 mean life: $\tau_{K_L^0}$	nsec	51.16 ± 0.21	51.7 ± 0.41	KLOE
$K_L^0 \rightarrow \pi^\pm e^\mp \nu_e$	10^{-2}	40.55 ± 0.11	38.78 ± 0.28	KLOE, KTeV
$K_L^0 \rightarrow \pi^\pm \mu^\mp \nu_\mu$	10^{-2}	27.04 ± 0.07	27.18 ± 0.25	KLOE, KTeV
$K_L^0 \rightarrow \pi^0 \pi^0 \pi^0$	10^{-2}	19.52 ± 0.12	21.13 ± 0.27	KLOE, KTeV
$K_L^0 \rightarrow \pi^+ \pi^- \pi^0$	10^{-2}	12.54 ± 0.05	12.55 ± 0.20	KLOE, KTeV
$K_L^0 \rightarrow \pi^+ \pi^-$	10^{-3}	1.966 ± 0.010	2.056 ± 0.033	KTeV
$K_L^0 \rightarrow \pi^0 \pi^0$	10^{-4}	8.65 ± 0.06	9.27 ± 0.19	KTeV
K_S^0 mean life: $\tau_{K_S^0}$	psec	89.53 ± 0.05	89.35 ± 0.08	KTeV, NA48
$K_S^0 \rightarrow \pi^0 \pi^0$	10^{-2}	30.69 ± 0.05	31.39 ± 0.28	KLOE
$K_S^0 \rightarrow \pi^+ \pi^-$	10^{-2}	69.20 ± 0.05	68.61 ± 0.28	KLOE
$K_S^0 \rightarrow \pi^\pm e^\mp \nu_e$	10^{-4}	7.04 ± 0.08	7.2 ± 1.4	NA48, KLOE
$ \epsilon $	10^{-3}	2.228 ± 0.011	2.271 ± 0.017	(from fit)
K^+ mass: m_{K^+}	MeV/ c^2	493.677 ± 0.016	493.677 ± 0.016	
K^+ mean life: τ_{K^+}	nsec	12.380 ± 0.021	12.386 ± 0.024	KLOE
$K^+ \rightarrow \mu^+ \nu_\mu$	10^{-2}	63.55 ± 0.11	63.51 ± 0.18	KLOE
$K^+ \rightarrow \pi^0 e^+ \nu_e$	10^{-2}	5.07 ± 0.04	4.28 ± 0.06	KLOE
$K^+ \rightarrow \pi^0 \mu^+ \nu_\mu$	10^{-2}	3.353 ± 0.034	3.18 ± 0.08	KLOE
$K^+ \rightarrow \pi^+ \pi^0$	10^{-2}	20.66 ± 0.08	21.16 ± 0.14	KLOE
$K^+ \rightarrow \pi^+ \pi^0 \pi^0$	10^{-2}	1.761 ± 0.022	1.73 ± 0.04	KLOE
$K^+ \rightarrow \pi^+ \pi^+ \pi^-$	10^{-2}	5.59 ± 0.04	5.59 ± 0.05	
$ V_{us} $		0.2252 ± 0.0009	0.2196 ± 0.0023	Section 9

* Decay modes mean their branching ratios.

8 Basic observables

Kaon decay experiments remeasured basic observables such as kaon masses, lifetimes, and absolute branching ratios. Features of the modern kaon experiments, with mature experimental methods, are the large statistics (high intensity of the beam and large acceptance of the detector), high resolution (state-of-the art and sophisticated techniques in the detector), advanced computing (for both data analysis and MC simulation), controlled systematic-uncertainties (e.g. simultaneous measurement of multiple decay modes) and better handling of the theoretical issues such as radiative corrections [174, 175, 176, 177, 178]. All of these are helpful in understanding the detector, background sources and uncertainties to do precise measurement of “(should-have-been) well-done” decays.

Instead of discussing each measurement, the values of basic observables taken from the books of Review of Particle Physics in 2010 [77] and in 2000 [179] are listed in table 4, to present how precisions were improved (or central values were significantly shifted) in the last ten years. It should also be mentioned that new measurements have come after Review of Particle Physics in 2010, for example on the K_S^0 mean life as $(89.562 \pm 0.029(stat.) \pm 0.043(syst.))$ psec from KLOE [180] and (89.623 ± 0.047) psec from KTeV [22].

It has been pointed out (e.g. [181, 182]) that an inconsistency exists in $|\epsilon|$ between the experimental value $((2.228 \pm 0.011) \times 10^{-3}$ in [77]) and the SM prediction $((1.81 \pm 0.28) \times 10^{-3}$ in [183]). This can be regarded as a tension between $|\epsilon|$ and $\sin 2\phi_1$ in the CKM-parameter fits, indicating hints for New Physics effects.

9 V_{us} and CKM unitarity

All the roads of kaon physics lead to CKM, in particular the V_{us} fountain, which was not built in a day. The magnitude of V_{us} , or λ in the Wolfenstein parametrization or $\sin \theta_C$ with the Cabibbo angle θ_C , is extracted from semileptonic kaon decays with

$$B(K_{\ell 3}) = \tau_K \times \frac{G_F^2 m_K^5}{192 \pi^3} C_K^2 S_{EW} \times |V_{us}|^2 \cdot f_+(0)^2 \times I_{K\ell} \left(1 + \delta_{EM}^{K\ell} + \delta_{SU(2)}^{K\pi} \right)^2 \quad (15)$$

$$\propto [|V_{us}| \cdot f_+(0)]^2 \quad (16)$$

or leptonic kaon decays with

$$\frac{B(K_{\ell 2})}{B(\pi_{\ell 2})} = \frac{\tau_K}{\tau_\pi} \times \frac{|V_{us}|^2}{|V_{ud}|^2} \cdot \frac{f_K^2}{f_\pi^2} \times \frac{m_K (1 - m_\ell^2/m_K^2)^2}{m_\pi (1 - m_\ell^2/m_\pi^2)^2} (1 + \delta_{EM}) \quad (17)$$

$$\propto \left[\frac{|V_{us}|}{|V_{ud}|} \cdot \frac{f_K}{f_\pi} \right]^2. \quad (18)$$

In Eq. 15, G_F is the Fermi constant, C_K^2 is 1 for K^0 decay and 1/2 for K^\pm decay, $S_{EW} = 1.0232(2)$ is the short-distance electroweak correction, $I_{K\ell}$ is a phase-space integral that is sensitive to the momentum dependence of the form factors, $\delta_{EM}^{K\ell}$ is the channel-dependent long-distance electromagnetic correction and $\delta_{SU(2)}^{K\pi}$ is the correction for isospin breaking (and is zero for K^0 decay) ¹⁶. In Eq. 17, $\delta_{EM} = -0.0070(18)$ is the long-distance electromagnetic correction that does not cancel from the ratio. What we obtain from the semileptonic and leptonic kaon-decay measurements are the values of $|V_{us}| \cdot f_+(0)$, where $f_+(0)$ is the $K \rightarrow \pi$ vector form factor at zero momentum transfer, and the product of the ratios $|V_{us}|/|V_{ud}|$ and f_K/f_π , where f_K and f_π are the kaon and pion decay constants, respectively. The values of $f_+(0)$ and f_K/f_π should be provided in order to extract $|V_{us}|$; they are obtained theoretically from lattice QCD calculations.

The $|V_{us}|$ results should satisfy one of the unitarity conditions of the CKM matrix elements, $|V_{ud}|^2 + |V_{us}|^2 + |V_{ub}|^2 = 1$. On the other hand, a new parameter Δ_{CKM} defined as

$$\Delta_{CKM} \equiv |V_{ud}|^2 + |V_{us}|^2 + |V_{ub}|^2 - 1 \quad (19)$$

is a benchmark to test the consistency of quark mixing in the SM. It had been pointed out that $|V_{us}| \simeq 0.220$ (the value in PDG2000, in table 4) led to $\Delta_{CKM} = (-3.2 \pm 1.4) \times 10^{-3}$ and indicated a two-sigma deviation from zero, until the BNL E865 experiment, whose main purpose was a search for $K^+ \rightarrow \pi^+ \mu^+ e^-$ [103], published a new measurement of $K^+ \rightarrow \pi^0 e^+ \nu$ [184] and claimed the branching ratio (and $|V_{us}|$) was larger. After that, more new results of precise branching-ratio measurements on neutral and charged kaon decays came (Section 8), and there have been laborious works in the collaboration of theorists and experimentalists, in particular by the FlaviaNet Kaon Working Group [185], to evaluate $|V_{us}|$ precisely. The latest achievements are described in details in [186], and a compact review is available in [187]. Instead of repeating these contents, the final values in [186] are summarized. The experimental result on $|V_{us}| \cdot f_+(0)$ is 0.2163(5) and, with $f_+(0) = 0.959(5)$, $|V_{us}|$ is 0.2254(13) from semileptonic kaon decays. The experimental result on $|V_{us}|/|V_{ud}| \cdot f_K/f_\pi$ is 0.2758(5) and, with $f_K/f_\pi = 1.193(6)$, $|V_{us}|/|V_{ud}|$ is 0.2312(13) from leptonic kaon decays. By using $|V_{ud}| = 0.97425(22)$, the combined $|V_{us}|$ is 0.2253(9) and Δ_{CKM} is $-0.0001(6)$.

The efforts on $|V_{ud}|$ will continue with the results from new kaon experiments.

¹⁶ $(1 + \delta_{EM}^{K\ell} + \delta_{SU(2)}^{K\pi})^2 \simeq (1 + 2 \delta_{EM}^{K\ell} + 2 \delta_{SU(2)}^{K\pi})$ is used in some papers.

10 Exotic searches

Experimental searches for very light bosons have a long history, but a neutral boson whose mass is twice the muon mass has not yet been excluded. In 2005, the HyperCP collaboration at FNAL reported three events of the $\Sigma^+ \rightarrow p\mu^+\mu^-$ decay, and the dimuon mass may indicate a neutral intermediate state P^0 with a mass of $214.3 \pm 0.5 \text{ MeV}/c^2$ [188]. Since the events were observed in an FCNC process with a strange to down quark transition, P^0 should be confirmable with kaon decays. Dimuon masses in previous $K^+ \rightarrow \pi^+\mu^+\mu^-$ measurements were not observed in the narrow range around the P^0 mass; thus, P^0 should be a pseudo-scalar or axial-vector particle and be studied with the three-body decay $K \rightarrow \pi\pi P^0$. The KTeV experiment searched for the $K_L^0 \rightarrow \pi^0\pi^0\mu^+\mu^-$ decay for the first time [189] and set $B(K_L^0 \rightarrow \pi^0\pi^0\mu^+\mu^-) < 9.2 \times 10^{-11}$ and $B(K_L^0 \rightarrow \pi^0\pi^0 P^0 \rightarrow \pi^0\pi^0\mu^+\mu^-) < 1.0 \times 10^{-10}$. The E391a experiment searched for a pseudoscalar particle X^0 in the decay $K_L^0 \rightarrow \pi^0\pi^0 X^0$, $X^0 \rightarrow \gamma\gamma$ in the mass range of X^0 from 194.3 to 219.3 MeV/c^2 , and set $B(K_L^0 \rightarrow \pi^0\pi^0 P^0 \rightarrow \pi^0\pi^0\gamma\gamma) < 2.4 \times 10^{-7}$ [190]. Both results almost ruled out the predictions that P^0 is a pseudo-scalar particle [191, 192].

The E787/E949 results on $K^+ \rightarrow \pi^+\nu\bar{\nu}$ have also been interpreted as a two-body decay $K^+ \rightarrow \pi^+U^0$, where U^0 is a massive non-interacting particle either stable or unstable, and as $K^+ \rightarrow \pi^+V^0$, $V^0 \rightarrow \nu\bar{\nu}$, for a hypothetical, short-lived particle V^0 . The limits are presented in [59]. Limits on the three-body decays $K^- \rightarrow \pi^-\pi^0 S^0$ and $K_L^0 \rightarrow \pi^0\pi^0 S^0$ were obtained in the ISTRA+ results [193] and in the E391a results [56], respectively, as searches for light pseudoscalar sgoldstino-particles S^0 [194]. The discovery potential of the rare FCNC kaon decays with *missing energy* in the final state is discussed recently in [195].

The NA48/2 experiment published the upper limit $B(K^\pm \rightarrow \pi^\mp\mu^\pm\mu^\pm) < 1.1 \times 10^{-9}$ [30]. This is a neutrino-less “double muon” decay by changing total lepton number by two, and provides a unique channel to search for effects of Majorana neutrinos in the second generation of quarks and leptons [196, 197].

The ISTRA+ experiment performed a search for a heavy neutrino in the mass from 40 to 80 MeV/c^2 and the lifetime from 10^{-11} to 10^{-9} in the $K^- \rightarrow \mu^-\nu_h \rightarrow \mu^-\nu\gamma$ decay, and put upper limits on the square of the mixing matrix element $|U_{\mu h}|^2$ [198]. Heavy neutrinos which are a part of the ν_μ flavor eigenstate and decay *radiatively* into a massless neutrino and a photon are considered as an explanation to the long-standing LSND/KARMEN/MiniBooNE anomaly in neutrino physics [199, 200, 201]. This decay can be studied with the detector which measures the $K \rightarrow \mu\nu\gamma$ decay.

The decay $K_L^0 \rightarrow 3\gamma$, which is forbidden by charge-conjugation invariance as in the case with $\pi^0 \rightarrow 3\gamma$, can proceed via parity-violating interactions without violating CP, but is further suppressed by the gauge invariance and Bose statistics [202]. E391a published the new upper limit $B(K_L^0 \rightarrow 3\gamma) < 7.4 \times 10^{-8}$ [203] on the assumption that the decay proceeded via parity-violation.

The decay $K^+ \rightarrow \pi^+\gamma$ is a spin $0 \rightarrow 0$ transition with a real photon and is thus forbidden by angular momentum conservation; it is also forbidden by gauge invariance. But this decay is allowed in noncommutative theories [204]. E949 published the upper limit $B(K^+ \rightarrow \pi^+\gamma) < 2.3 \times 10^{-9}$ [205].

11 Conclusion

The study of kaon physics continues to make great strides. The current program to study CP violation is being completed; the CP violation in $Re(\epsilon'/\epsilon)$ was established, but the CP asymmetries in charged kaon decays have not been observed yet. The rare decays $K_L^0 \rightarrow \pi^0 \nu \bar{\nu}$ and $K^+ \rightarrow \pi^+ \nu \bar{\nu}$, the transverse muon polarization in K^+ decays at rest and the lepton flavor universality in $\Gamma(K^+ \rightarrow e^+ \nu(\gamma))/\Gamma(K^+ \rightarrow \mu^+ \nu(\gamma))$ will be measured in a new series of experiments. Tests of CPT and quantum mechanics will continue in ϕ factory experiments. New results on radiative kaon decays, $\pi\pi$ scattering lengths, Dalitz-plot densities, form factors, basic observables, V_{us} , and exotic decays have been reported, and their measurements will continue in new experiments. The kaon experiments, with ultra-high sensitivities and precisions, will continue to be essential and crucial as a probe of New Physics beyond the Standard Model.

Acknowledgments

I would like to thank B. Bloch-Devaux, E. Blucher, F. Bossi, A.J. Buras, A. Ceccucci, A. Di Domenico, V.A. Duk, E. Goudzovski, G. Isidori, L.S. Littenberg, F. Mescia, M. Moulson, C. Smith, and T. Yamanaka for providing me help with this article. I would like to acknowledge support from Grant-in-Aids for Scientific Research on Priority Areas: "New Developments of Flavor Physics" and for Scientific Research (S) by the MEXT Ministry of Japan.

This article is dedicated to the memory of my wife, Yuko Nitta-Komatsubara, who passed away on March 21, 2011.

References

- [1] G.D. Rochester and C.C. Butler, *Nature* 160 (1947) 855
- [2] Edited by J.L. Rosner and B.D. Winstein, *Kaon Physics* (The University of Chicago Press, 2001)
- [3] T.K. Komatsubara, arXiv:hep-ex/0112016, in the Proceedings of the XXI Physics in Collision conference
- [4] T.K. Komatsubara, arXiv:hep-ex/0501016, in the Proceedings of FPCP2004
- [5] T.K. Komatsubara, arXiv:1006.4269, in the Proceedings of LEPTON PHOTON 2009
- [6] V. Cirigliano, G. Ecker, H. Neufeld, A. Pich, and J. Portolés, arXiv:1107.6001
- [7] A.J. Buras, arXiv:1102.5650
- [8] FLAG working group of FLAVIANET, G. Colangelo *et al.*, *Eur. Phys. J. C* 71 (2011) 1695
- [9] G. Buchalla, T.K. Komatsubara, F. Muheim, L. Silvestrini (Convenors) *et al.*, Report of Working Group 2 of the CERN Workshop “Flavor in the era of the LHC”, *Eur. Phys. J. C* 57 (2008) 309
- [10] J.H. Christenson, J.W. Cronin, V.L. Fitch, and R. Turlay, *Phys. Rev. Lett.* 13 (1964) 138
- [11] V.L. Fitch, *Rev. Mod. Phys.* 53 (1981) 367
- [12] J.W. Cronin, *Rev. Mod. Phys.* 53 (1981) 373
- [13] L. Wolfenstein, *Phys. Rev. Lett.* 13 (1964) 562
- [14] M. Kobayashi and T. Maskawa, *Prog. Theor. Phys.* 49 (1973) 652
- [15] M. Kobayashi, *Rev. Mod. Phys.* 81 (2009) 1019
- [16] T. Maskawa, *Rev. Mod. Phys.* 81 (2009) 1027
- [17] CPLEAR Collaboration, A. Angelopoulos *et al.*, *Phys. Rep.* 374 (2003) 165
- [18] K. Anikeev *et al.*, Report of the Workshop on B Physics at the Tevatron Run II and Beyond, arXiv:hep-ph/0201071
- [19] L.S. Littenberg, *Phys. Rev. D* 39 (1989) 3322
- [20] Y. Grossman and Y. Nir, *Phys. Lett. B* 398 (1997) 163
- [21] J. R. Batley *et al.*, *Phys. Lett. B* 544 (2002) 97
- [22] E. Abouzaid *et al.*, *Phys. Rev. D* 83 (2011) 092001
- [23] The NA48 Collaboration, V. Fanti *et al.*, *Nucl. Instrum. Methods. Phys. Res. Sect. A* 574 (2007) 433
- [24] The NA48 Collaboration, A. Lai *et al.*, *Eur. Phys. J. C* 22 (2001) 231
- [25] KTeV Collaboration, A. Alavi-Harati *et al.*, *Phys. Rev. D* 67 (2003) 012005
- [26] E. Blucher, B. Winstein, and T. Yamanaka, *Prog. Theor. Phys.* 122 (2009) 81
- [27] T.G. Trippe, *Dalitz Plot Parameters for $K \rightarrow 3\pi$ Decays* (1999), in *Review of Particle Physics* (2010)
- [28] The NA48/2 Collaboration, J. R. Batley *et al.*, *Eur. Phys. J. C* 52 (2007) 875
- [29] NA48/2 Collaboration, J.R. Batley *et al.*, *Phys. Lett. B* 677 (2009) 246
- [30] NA48/2 Collaboration, J.R. Batley *et al.*, *Phys. Lett. B* 697 (2011) 107
- [31] The NA48/2 Collaboration, J.R. Batley *et al.*, *Eur. Phys. J. C* 68 (2010) 75
- [32] S. L. Glashow, J. Iliopoulos, and L. Maiani, *Phys. Rev. D* 2 (1970) 1285
- [33] M.K. Gaillard and B.W. Lee, *Phys. Rev. D* 10 (1974) 897
- [34] T. Inami and C.S. Lim, *Prog. Theor. Phys.* 65 (1981) 297 ; 65 (1981) 1172(E)
- [35] E787 Collaboration, S. Adler *et al.*, *Phys. Rev. Lett.* 79 (1997) 2204

- [36] L. Wolfenstein, *Phys. Rev. Lett.* 51 (1983) 1945
- [37] N. Cabibbo, *Phys. Rev. Lett.* 10 (1963) 531
- [38] M.S. Sozzi, arXiv:1102.0893
- [39] A.J. Buras, S. Uhlig, and F. Schwab, *Rev. Mod. Phys.* 80 (2008) 965
- [40] J. Brod, M. Gorbahn, and E. Stamou, *Phys. Rev. D* 83 (2011) 034030
- [41] F. Mescia and C. Smith, *Phys. Rev. D* 76 (2007) 034017
- [42] A.J. Buras, M. Gorbahn, U. Haisch, and U. Nierste, *J. High Energy P.* 0611 (2006) 002
- [43] J. Brod and M. Gorbahn, *Phys. Rev. D* 78 (2008) 034006
- [44] D. Bryman, A.J. Buras, G. Isidori, and L. Littenberg, *Int. J. Mod. Phys. A* A21 (2006) 487
- [45] F. Mescia and C. Smith, *K $\rightarrow \pi \nu \nu$ decay in the Standard Model*,
<http://www.lnf.infn.it/wg/vus/content/Krare.html>
- [46] A.J. Buras, *Acta Physica Polonica B* 41 (2010) 2487
- [47] D.M. Straub, arXiv:1012.3893
- [48] M. Gorbahn, M. Patel and S. Robertson, arXiv:1104.0826
- [49] H. Watanabe *et al.*, *Nucl. Instrum. Methods. Phys. Res. Sect. A* 545 (2005) 542
- [50] M. Doroshenko *et al.*, *Nucl. Instrum. Methods. Phys. Res. Sect. A* 545 (2005) 278
- [51] Y. Tajima *et al.*, *Nucl. Instrum. Methods. Phys. Res. Sect. A* 592 (2008) 261
- [52] R. Ogata for the E391a Collaboration, *Nucl. Instrum. Methods. Phys. Res. Sect. A* 623 (2010) 243
- [53] E391a Collaboration, J.K. Ahn *et al.*, *Phys. Rev. D* 81 (2010) 072004
- [54] A. Alavi-Harati *et al.*, *Phys. Rev. D* 61 (2000) 072006
- [55] KTeV Collaboration, J. Adams *et al.*, *Phys. Lett. B* 447 (1999) 240
- [56] E391a Collaboration, R. Ogata *et al.*, *Phys. Rev. D* 84 (2011) 052009
- [57] J. Doornbos *et al.*, *Nucl. Instrum. Methods. Phys. Res. Sect. A* 444 (2000) 546
- [58] S. Adler *et al.*, *Phys. Rev. D* 77 (2008) 052003
- [59] E949 Collaboration, A.V. Artamonov *et al.*, *Phys. Rev. D* 79 (2009) 092004
- [60] E787 Collaboration, S. Adler *et al.*, *Phys. Rev. D* 63 (2001) 032004
- [61] <http://koto.kek.jp/>
- [62] H. Nanjo for the J-PARC E14 K^OTO Collaboration, *PoS KAON09* (2009) 047
- [63] H. Watanabe for the J-PARC E14 K^OTO Collaboration, *PoS ICHEP 2010* (2010) 274
- [64] <http://j-parc.jp/>
- [65] http://j-parc.jp/researcher/Hadron/en/Proposal_e.html
- [66] T. Shimogawa for the J-PARC E14 K^OTO Collaboration, *Nucl. Instrum. Methods. Phys. Res. Sect. A* 623 (2010) 585
- [67] H. Takahashi *et al.*, *J. Phys. Conf. Ser.* 312 (2011) 052027
- [68] K. Shiomi *et al.*, *Nucl. Instrum. Methods. Phys. Res. Sect. A* 664 (2012) 264
- [69] G. Takahashi *et al.*, *Jpn. J. Appl. Phys.* 50 (2011) 036701
- [70] <http://na62.web.cern.ch/NA62/>
- [71] T. Spadaro, arXiv:1101.5631
- [72] NA62 Collaboration, *NA62 Technical Design* (2010),
<http://na62.web.cern.ch/NA62/Documents/ReferenceDocuments.html>

- [73] P. Valente on behalf of the NA62 Collaboration, *A detector for the measurement of the ultrarare decay $K^+ \rightarrow \pi^+ \nu \nu$: NA62 at the CERN SPS*, presented at the 2011 Europhysics Conference in High Energy Physics
- [74] <http://projectx.fnal.gov/>
- [75] R. Tschirhart, arXiv:1109.3500
- [76] <http://www.intensityfrontier.org/>
- [77] K. Nakamura *et al.* (Particle Data Group), *J. Phys. G* 37 (2010) 075021 and 2011 partial update for the 2012 edition, <http://pdg.lbl.gov/>
- [78] L.M. Sehgal, *Phys. Rev.* 183 (1969) 1511
- [79] G. Isidori and R. Unterdorfer, *J. High Energy P.* 0401 (2004) 009
- [80] KLOE Collaboration, F. Ambrosino *et al.*, *Phys. Lett. B* 672 (2009) 203
- [81] G. Buchalla, G. D'Ambrosio, G. Isidori, *Nucl. Phys. B* 672 (2003) 387
- [82] G. Isidori, C. Smith, R. Unterdorfer, *Eur. Phys. J. C* 36 (2004) 57
- [83] P. Mertens and C. Smith, *J. High Energy P.* 1108 (2011) 069
- [84] A. Lai *et al.*, *Phys. Lett. B* 536 (2002) 229
- [85] E. Abouzaid *et al.*, *Phys. Rev. D* 77 (2008) 112004
- [86] F. Mescia, C. Smith, S. Trine, *J. High Energy P.* 0608 (2006) 088
- [87] J.R. Batley *et al.*, *Phys. Lett. B* 576 (2003) 43
- [88] J.R. Batley *et al.*, *Phys. Lett. B* 599 (2004) 197
- [89] H.B. Greenlee, *Phys. Rev. D* 42 (1990) 3724
- [90] A. Alavi-Harati *et al.*, *Phys. Rev. Lett.* 93 (2004) 021805
- [91] A. Alavi-Harati *et al.*, *Phys. Rev. Lett.* 84 (2000) 5279
- [92] I.I. Bigi and A.I. Sanda, *CP violation, Second Edition* (Cambridge University Press, 2009)
- [93] R. Garisto and G. Kane, *Phys. Rev. D* 44 (1991) 2038
- [94] J.A. Macdonald *et al.*, *Nucl. Instrum. Methods. Phys. Res. Sect. A* 506 (2003) 60
- [95] E246 Collaboration, M. Abe *et al.*, *Phys. Rev. D* 73 (2006) 072005
- [96] E246 Collaboration, V.V. Anisimovsky *et al.*, *Phys. Lett. B* 562 (2003) 166
- [97] <http://trek.kek.jp/>
- [98] J. Imazato, *PoS KAON09* (2009) 007
- [99] R.N. Cahn and H. Harari, *Nucl. Phys. B* 176 (1980) 135
- [100] O. Shanker, *Nucl. Phys. B* 206 (1982) 253
- [101] B.A. Campbell, *Phys. Rev. D* 28 (1983) 209
- [102] MEG Collaboration, J. Adam *et al.*, *Phys. Rev. Lett.* 107 (2011) 171801
- [103] A. Sher *et al.*, *Phys. Rev. D* 72 (2005) 012005
- [104] KTeV Collaboration, E. Abouzaid *et al.*, *Phys. Rev. Lett.* 100 (2008) 131803
- [105] V. Cirigliano and I. Rosell, *Phys. Rev. Lett.* 99 (2007) 231801
- [106] A. Masiero, P. Paradisi, and R. Petronzio, *Phys. Rev. D* 74 (2006) 011701(R)
- [107] A. Masiero, P. Paradisi, and R. Petronzio, *J. High Energy P.* 0811 (2008) 042
- [108] <http://pienu.triumf.ca/>
- [109] <http://pen.phys.virginia.edu/>
- [110] KLOE Collaboration, F. Bossi *et al.*, *Riv. Nuovo Cim.* 31 (2008) 531

- [111] J. Lee-Franzini and P. Franzini, *Acta Physica Polonica B* 38 (2007) 2703
- [112] P. Franzini and M. Moulson, *Ann. Rev. Nucl. Part. Sci.* 56 (2006) 207
- [113] KLOE Collaboration, F. Ambrosino *et al.*, *Eur. Phys. J. C* 64 (2009) 627 ; C65 (2010) 703(E)
- [114] KLOE Collaboration, presented by M. Moulson, PoS KAON09 (2009) 035
- [115] NA62 Collaboration, C. Lazzeroni *et al.*, *Phys. Lett. B* 698 (2011) 105
- [116] E. Goudzovski on behalf of the NA48 and NA62 collaborations, arXiv:1111.2818
- [117] J-PARC E06 TREK Collaboration, C. Rangacharyulu *et al.*, *Measurement of $\Gamma(K^+ \rightarrow e^+)/\Gamma(K^+ \rightarrow \mu^+\nu)$ and Search for heavy sterile neutrinos using the TREK detector system* (2010)
- [118] The KLOE collaboration, G. D'Ambrosio and G. Isidori, *J. High Energy P.* 0612 (2006) 011
- [119] M. Antonelli and G. D'Ambrosio, *CPT Invariance Tests in Neutral Kaon Decay* (2009), in *Review of Particle Physics* (2010)
- [120] KLOE Collaboration, F. Ambrosino *et al.*, *Phys. Lett. B* 642 (2006) 315
- [121] A. Di Domenico and the KLOE collaboration, *J. Phys. Conf. Ser.* 171 (2009) 012008
- [122] A. Di Domenico, PoS KAON09 (2009) 038
- [123] <http://www.lnf.infn.it/kloe2/>
- [124] G. Amelino-Camelia *et al.*, *Eur. Phys. J. C* 68 (2010) 619
- [125] P. Raimondi, D. Shatilov, M. Zobov, arXiv:physics/0702033
- [126] M. Zobov *et al.*, *Phys. Rev. Lett.* 104 (2010) 174801
- [127] KLOE-2 Collaboration, G. De Robertis *et al.*, arXiv:1002.2572
- [128] C. Bloise on behalf of the KLOE-2 Collaboration, *Kaon physics at KLOE and KLOE-2 prospects*, presented at the 2011 Europhysics Conference in High Energy Physics
- [129] D. Moricciani on behalf of the KLOE-2 collaboration, *The KLOE-2 detector upgrade at DAΦNE*, presented at the 2011 Europhysics Conference in High Energy Physics
- [130] R.H. Dalitz, *Proc. Phys. Soc. London Sect. A* 64 (1951) 667
- [131] S. Weinberg, *Physica A* 96 (1979) 327
- [132] S. Weinberg, arXiv:0908.1964
- [133] J. Gasser and H. Leutwyler, *Ann. Phys. (N.Y.)* 158 (1984) 142
- [134] J. Gasser and H. Leutwyler, *Nucl. Phys. B* 250 (1985) 465
- [135] J.F. Donoghue, E. Golowich, and B.R. Holstein, *Dynamics of the Standard Model* (Cambridge University Press, 1992)
- [136] Edited by L. Maiani, G. Pancheri, and N. Paver, *The DAΦNE Physics Handbook* (LNFN, 1992)
- [137] The KLOE Collaboration, F. Ambrosino *et al.*, *Eur. Phys. J. C* 55 (2008) 539
- [138] KTeV Collaboration, E. Abouzaid *et al.*, *Phys. Rev. Lett.* 99 (2007) 081803
- [139] KTeV Collaboration, E. Abouzaid *et al.*, *Phys. Rev. D* 76 (2007) 052001
- [140] E. Abouzaid *et al.*, *Phys. Rev. Lett.* 99 (2007) 051804
- [141] NA48/1 Collaboration, J.R. Batley *et al.*, *Phys. Lett. B* 694 (2011) 301
- [142] The KLOE Collaboration, F. Ambrosino *et al.*, *J. High Energy P.* 0805 (2008) 051
- [143] S.A. Akimenko *et al.*, *Phys. Atom. Nucl.* 70 (2007) 702
- [144] E787 Collaboration, S. Adler *et al.*, *Phys. Rev. D* 81 (2010) 092001
- [145] O.G. Tchikilev *et al.*, *Phys. Atom. Nucl.* 70 (2007) 29
- [146] NA48/2 Collaboration, J.R. Batley *et al.*, *Phys. Lett. B* 659 (2008) 493
- [147] V.A. Duk *et al.*, *Phys. Lett. B* 695 (2011) 59

- [148] V. Kurshetsov, *PoS KAON09* (2009) 051
- [149] G. Colangelo, J. Gasser, H. Leutwyler, *Phys. Lett. B* 488 (2000) 261
- [150] G. Colangelo, J. Gasser, H. Leutwyler, *Nucl. Phys. B* 603 (2001) 125
- [151] B. Adeva *et al.*, *Phys. Lett. B* 704 (2011) 24
- [152] N. Cabibbo, *Phys. Rev. Lett.* 93 (2004) 121801
- [153] N. Cabibbo, G. Isidori, *J. High Energy P.* 0503 (2005) 021
- [154] G. Colangelo, J. Gasser, B. Kubis, A. Rusetsky, *Phys. Lett. B* 638 (2006) 187
- [155] S.R. Gevorkyan, A.V. Tarasov, O.O. Voskresenskaya, *Phys. Lett. B* 649 (2007) 159
- [156] M. Bissegger, A. Fuhrer, J. Gasser, B. Kubis, A. Rusetsky, *Nucl. Phys. B* 806 (2009) 178
- [157] J.R. Batley *et al.*, *Eur. Phys. J. C* 64 (2009) 589
- [158] S. Pislak *et al.*, *Phys. Rev. D* 67 (2003) 072004 ; D 81 (2010) 119903(E)
- [159] L. Rosselet *et al.*, *Phys. Rev. D* 15 (1977) 574
- [160] A. Pais and S.B. Treiman, *Phys. Rev.* 168 (1968) 1858
- [161] B. Ananthanarayan, G. Colangelo, J. Gasser, H. Leutwyler, *Phys. Rep.* 353 (2001) 207
- [162] S. Descotes, N.H. Fuchs, L. Girlanda, J. Stern, *Eur. Phys. J. C* 24 (2002) 469
- [163] S. Roy, *Phys. Lett. B* 36 (1971) 353
- [164] G. Colangelo, J. Gasser, A. Rusetsky, *Eur. Phys. J. C* 59 (2009) 777
- [165] The NA48/2 Collaboration, J.R. Batley *et al.*, *Eur. Phys. J. C* 70 (2010) 635
- [166] NA48/2 Collaboration, J.R. Batley *et al.*, *Phys. Lett. B* 686 (2010) 101
- [167] NA48/2 Collaboration, J.R. Batley *et al.*, *Phys. Lett. B* 649 (2007) 349
- [168] B. Bloch-Devaux on behalf of the NA48/2 collaboration, *Study of K_{e4} decays in the NA48/2 experiment at CERN*, presented at the 46th Rencontres de Moriond 2011 QCD and High Energy Interactions
- [169] KTeV Collaboration, E. Abouzaid *et al.*, *Phys. Rev. D* 78 (2008) 032009
- [170] KLOE Collaboration, F. Ambrosino *et al.*, *Phys. Lett. B* 636 (2006) 166
- [171] KTeV Collaboration, E. Abouzaid *et al.*, *Phys. Rev. D* 81 (2010) 052001
- [172] The KLOE collaboration, F. Ambrosino *et al.*, *J. High Energy P.* 0712 (2007) 105
- [173] NA48 Collaboration, A. Lai *et al.*, *Phys. Lett. B* 647 (2007) 341
- [174] C. Gatti, *Eur. Phys. J. C* 45 (2006) 417
- [175] E. Baracchini, G. Isidori, *Phys. Lett. B* 633 (2006) 309
- [176] T.C. André, *Ann. Phys. (N.Y.)* 322 (2007) 2518
- [177] G. Nanava, Z. Was, *Eur. Phys. J. C* 51 (2007) 569
- [178] V. Cirigliano, arXiv:hep-ph/0606020
- [179] D.E. Groom *et al.* (Particle Data Group), *Eur. Phys. J. C* 15 (2000) 1
- [180] The KLOE collaboration, F. Ambrosino *et al.*, *Eur. Phys. J. C* 71 (2011) 1604
- [181] E. Lunghi, A. Soni, *Phys. Lett. B* 666 (2008) 162
- [182] A.J. Buras and D. Guadagnoli, *Phys. Rev. D* 78 (2008) 033005
- [183] J. Brod and M. Gorbahn, arXiv:1108.2036
- [184] A. Sher *et al.*, *Phys. Rev. Lett.* 91 (2003) 261802
- [185] <http://www.lnf.infn.it/wg/vus/>
- [186] M. Antonelli *et al.* for the FlaviaNet Working Group on Kaon Decay, *Eur. Phys. J. C* 69 (2010) 399

- [187] E. Blucher and W.J. Marciano, V_{ud} , V_{us} the Cabibbo Angle, and CKM Unitarity (2009), in *Review of Particle Physics* (2010)
- [188] HyperCP Collaboration, H.K. Park *et al.*, *Phys. Rev. Lett.* 94 (2005) 021801
- [189] The KTeV Collaboration, E. Abouzaid *et al.*, *Phys. Rev. Lett.* 107 (2011) 201803
- [190] E391a Collaboration, Y.C. Tung *et al.*, *Phys. Rev. Lett.* 102 (2009) 051802
- [191] X.G. He, J. Tandean, and G. Valencia, *Phys. Rev. Lett.* 98 (2007) 081802
- [192] S. Oh and J. Tandean, *J. High Energy P.* 1001 (2010) 022
- [193] O.G. Tchikilev *et al.*, *Phys. Lett. B* 602 (2004) 149
- [194] D.S. Gorbunov and V.A. Rubakov, *Phys. Rev. D* 64 (2001) 054008
- [195] J.F. Kamenik and C. Smith, arXiv:1111.6402
- [196] K. Zuber, *Phys. Lett. B* 479 (2000) 33
- [197] L.S. Littenberg and R.E. Shrock, *Phys. Lett. B* 491 (2000) 285
- [198] V.A. Duk *et al.*, arXiv:1110.1610
- [199] S.N. Gninenko, *Phys. Rev. Lett.* 103 (2009) 241802
- [200] S.N. Gninenko, *Phys. Rev. D* 83 (2011) 015015
- [201] S.N. Gninenko, *Phys. Rev. D* 83 (2011) 093015
- [202] C.N. Yang, *Phys. Rev.* 77 (1950) 242
- [203] E391a Collaboration, Y.C. Tung *et al.*, *Phys. Rev. D* 83 (2011) 031101(R)
- [204] B. Melić, K. Passek-Kumerički, and J. Trampetić, *Phys. Rev. D* 72 (2005) 057502
- [205] E949 Collaboration, A.V. Artamonov *et al.*, *Phys. Lett. B* 623 (2005) 192